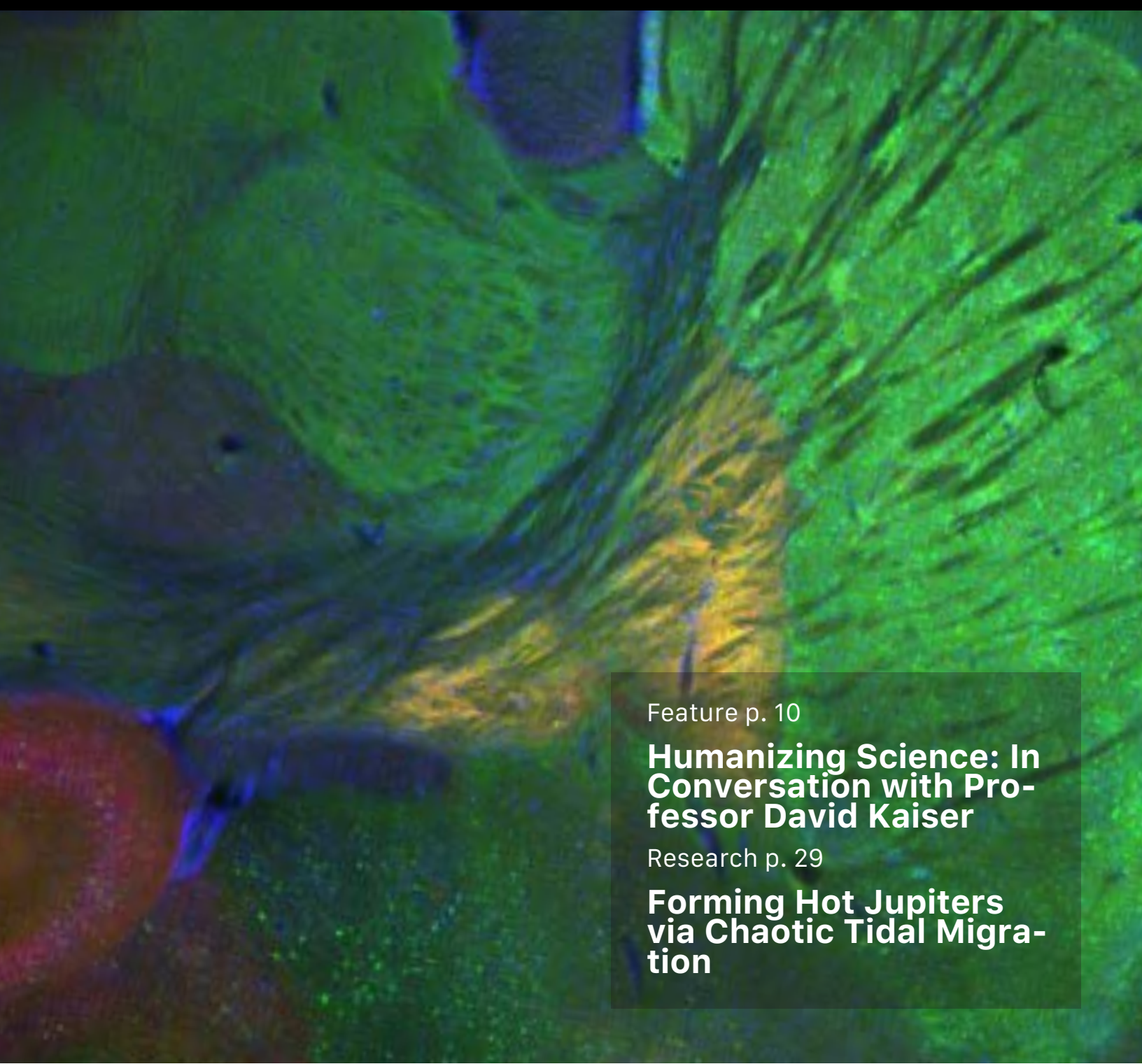


# MURJ

Massachusetts Institute of Technology  
Undergraduate Research Journal



Feature p. 10

**Humanizing Science: In  
Conversation with Pro-  
fessor David Kaiser**

Research p. 29

**Forming Hot Jupiters  
via Chaotic Tidal Migra-  
tion**

# Diverse minds, bold disruptors, meaningful impact.

## 290 Binney Street

Nestled in the heart of the world's top center for biotech and tech innovation will soon lie 290 Binney Street – AstraZeneca's global strategic R&D site – designed to inspire great minds, disrupt science and transform patients' lives.

Scan the QR code below to see the opportunities waiting for you.





# Contents

---

## INTRODUCTORY LETTER

- 2 From the Editor

## NEWS

- 4 **The Climate for Climate Research at MIT**  
Logan Reich

## FEATURES

- 10 **Humanizing Science: In Conversation with Professor David Kaiser**  
Charlotte Myers
- 13 **Turning the Tide: Combining Nanoparticles and Immunotherapy to Fight Pancreatic Cancer**  
Cindy (Subin) Pyo

## SPOTLIGHTS

- 17 **Esme Sun**
- 18 **Victory Yinka-Banjo**

## UROP SUMMARIES

- 20 **Mapping Mindfulness: A Systematic Review of the Neuroanatomy Associated with Mindfulness**  
Kannammai Pichappan, Isaac Treves, John Gabrieli
- 25 **Empowering Student Wellbeing Through Technology: Insights from a Digital Phenotyping Study on Stress and Sleep Quality**  
Ariadne Dulchinos, Edwin Ouko, Sabrina Do, Valerie Kwek, Somaia Saba, Richard Fletcher
- 29 **Forming Hot Jupiters via Chaotic Tidal Migration**  
Donald Liveoak, Sarah Millholland
- 32 **Barriers to Innovation: An Interview-Based Study of Opioid Startups and Industry Stakeholders**  
Riley Davis, Vivian Lee, David Santana, Zen Chu, Freddy Nguyen
- 34 **Trust-building Hierarchical Automation: Validating the Transfer of Perovskite Properties Across Scales**  
Kanokwan Tungkitkancharoen, Alexander Siemenn, Professor Tonio Buonassisi

## REPORTS

- 39 **Depth-first search for tensor rank and border rank over finite fields**  
Jason Yang, Virginia Vassilevska Williams
- 44 **Deep-Sea Sediment Sampler for Hadal Depths**  
Audrey Chen, Jessica Lam, Thao Do, Ansel J Garcia-Langley, Ved Ganesh, Andrew Bennett, Michael Triantafyllou



UNDERGRADUATE  
RESEARCH JOURNAL  
Volume 48, Fall 2024

**Editor-in-Chief**  
Lia Bu

**Content Editor**  
Charlotte Myers

**Research Editor**  
Ananth Shyamal

**Layout Chief**  
Anna Dong

**Treasurer**  
Anna Dong

**Webmaster**  
Gwyneth Tangog

**MURJ Staff**  
MIT Undergraduate Research Journal

**Massachusetts  
Institute of Technology**

November 2024

Dear MIT Community,

The MURJ team is pleased to publish the 48th issue of the MIT Undergraduate Research Journal (MURJ). A biannual, student-led publication, the issue features innovative undergraduate research at MIT and highlights community and other aspects of the MIT population. In this issue, we are especially excited to share a new feature: the research spotlight, which emphasizes the background and contributions of exceptional MIT undergraduate researchers. Throughout this particular publication, we are reminded of the people behind all types of research, and seek to recognize their backgrounds and contributions.

Research in this issue spans a variety of fields, including math, electrical engineering, mechanical engineering, neuroscience, computer science, cognitive science, and physics. We are happy to be able to highlight the diversity of undergraduate research at MIT, from exploring the planets and stars to how sleep can better improve student wellbeing on campus. All projects are incredibly impactful on the MIT community and demonstrate the capability of students to contribute to an advancement of scientific knowledge and improvement of society. Through our new research spotlight, we especially recognize Victory Yinka-Banjo (MIT '25, Course 6-7) and Esme Sun (MIT '25, Course 6-7) for their exceptional work within computational biology and gene editing, respectively.

In addition to highlighting the undergraduate research conducted on campus, we share updates from the MIT community spanning the new MIT Climate Project, to an interview with Professor David Kaiser, the Germeshausen Professor of the

---

No material appearing in this publication may be reproduced without written permission of the publisher. The opinions expressed in this magazine are those of the contributors and are not necessarily shared by the editors. All editorial rights are reserved.

Massachusetts  
Institute of Technology

MURJ Staff  
MIT Undergraduate Research Journal



UNDERGRADUATE  
RESEARCH JOURNAL  
Volume 48, Fall 2024

History of Science and Professor of Physics discussing the humanization of science. These interviews remind us of the importance of the human element present in research, which can at times be forgotten.

The publication and distribution of this research would not be possible without a great collaborative effort: we thank the undergraduate researchers, their mentors, and professors for their work and dedication towards scientific research. In addition, I wish to highlight the dedicated work of the MURJ content, research, and layout staff, without whom this publication would not be possible. We also thank you, the reader, for choosing to learn about the incredible accomplishments and events occurring in the MIT community.

If you have any questions or would like to learn more, please reach out to [murj-officers@mit.edu](mailto:murj-officers@mit.edu).

All the best,

Lia Pascale Bu  
Editor-in-Chief  
Chemical Engineering | Class of 2025

### Content Staff

Cindy Pyo  
Logan Reich  
Annette Vega

### Research Staff

Angie Ayoubi  
Olivia Bartrum  
Eugenie Cha  
Sophia Chen  
Elizabeth Costa  
Isabella He  
Anthony Lin  
Diya Ramesh

### Layout Staff

Julia Cherchever  
Isabella He  
Annette Vega

---

No material appearing in this publication may be reproduced without written permission of the publisher. The opinions expressed in this magazine are those of the contributors and are not necessarily shared by the editors. All editorial rights are reserved.

## ENVIRONMENTAL SCIENCES

# The Climate for Climate Research at MIT

*The newly inaugurated MIT climate project helps catalyze and unify climate adaptation and mitigation research at MIT.*

By Logan Reich

The Climate Project is a new, large-scale effort by MIT to support climate research, encompassing the work of over 300 professors and promising over \$75 million in funding to accelerate these research efforts. Climate research at MIT spans a broad range from policy research, to creating more sustainable materials, and improving models of climate processes. The goal of the Climate Project is not to override these varied groups, but instead to “provide a new opportunity for MIT faculty, researchers, and students to be part of mission-driven problem-solving communities, focused on addressing what they see as some of the key gaps in the global climate response,” as well as to help support them with resources, according to Tom Kiley, a senior advisor in the recently created Office of the Vice President for Climate. “The goal of the Climate Project is to enable us to do the bigger things faster, and identify and develop rapidly scalable solutions”, Kiley says. Structurally, it is divided into six missions, each representing a key area of climate research, and corresponding to a strength in MIT’s capabilities.

*“Responsible research and teaching requires input and expertise from across the fields of science, engineering, humanities, and the social sciences, as well as working with partners beyond academia.”*

Professor Benedetto Marelli heads up the Wild Cards mission, which looks to identify “high risk, high payoff” technologies for the climate field, according to Professor Marelli in the Civil and Environmental Engineering Department. Personally, his research focuses on the application of biopolymers to mitigating the impacts of climate change. These biopolymers can be created from transforming food waste, textile manufacturing byproducts, and natural materials into technical materials with more useful properties

for applications, especially increased durability. Silk is a key base for many of these developing materials, creating films, tubes, and hydrogels, with so many applications that Marelli says it is becoming a “platform technology”. The goal is to apply these silk-derived biopolymers to uses ranging from edible food packaging, to fertilizer storage and release, to removing PFAS (per- and polyfluoroalkyl substances, a widespread pollutant). These applications are unified by the goal of reducing emissions and improving sustainability in small steps that can have large applications when scaled up.

That scaling is what the Climate Project really focuses on, by supporting researchers to start thinking about the large-scale applications and impact of research before the work has even started. This is an area where Professor Marelli already has experience, having spun out the silk-based edible coating research into a startup called Mori. The goal is to replicate this success with other developing technologies, potentially including technologies created by students, as new and innovative ideas are a centerpiece of the Wild Cards mission.

Not all climate research is focused on engineering, however, and not all of it lies under the umbrella of the Climate Project, at least not yet. Professor Raffaele Ferrari in the Earth, Atmosphere, and Planetary Sciences (EAPS) Department focuses on advancing climate modeling. Climate models, or earth systems models, are extremely complex simulations incorporating ocean, atmospheric, and land based processes to model the development of the overall climate. As of now, these models still possess a great amount of uncertainty, largely due to limited processing power forcing small-scale processes, such as cloud formation, to be approximated very roughly, greatly increasing model variability.

Cutting-edge climate models can only resolve scales on the order of tens to hundreds of kilometers and use approximate algorithms to capture the climate impact of smaller-scale important processes like vortex formations in the



# People. Passion. Possibilities.®

For ten years, we've dedicated ourselves to making a difference in people's lives. Creating medicines and solutions that help patients, communities, and our world. Because you are at the heart of what we do.



*Belcher, Jake. MIT Climate Summit Image. MIT News, 2024, [https://news.mit.edu/sites/default/files/download/202409/MIT-Climate%20Summit\\_JakeBelcher-03-PRESS.jpg](https://news.mit.edu/sites/default/files/download/202409/MIT-Climate%20Summit_JakeBelcher-03-PRESS.jpg).*

ocean and small weather systems in the atmosphere. The algorithms depend on unknown parameters that are fitted to reproduce the climate evolution over the past century. The Climate Modeling Alliance, which Professor Ferrari is part of, is working on building a new climate model that is more computationally efficient, leveraging more modern languages and computational techniques, to capture a larger fraction of small-scale processes. This new model will also improve on uncertainty estimation, which current climate models are poor at, by calibrating unknown parameters with massive amount of data routinely collected by satellites, atmospheric balloons, and ocean ships and floats. Quantifying the uncertainty is key towards understanding the validity of model predictions and the associated policy decisions.

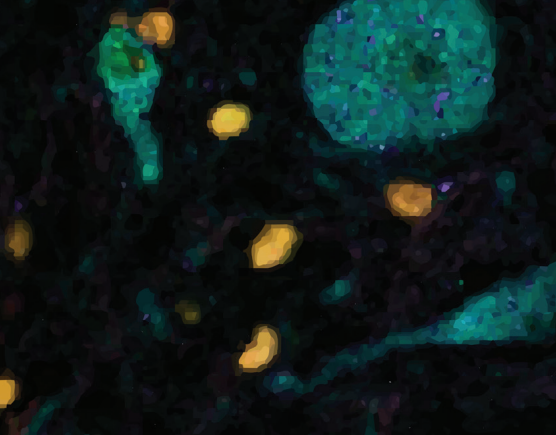
On top of building this new model, Professor Ferrari is also working on using machine learning and other algorithmic approximation techniques in order to allow for less computationally intensive models called emulators to approximate the results of the complex climate models and allow them to consider a wide range of potential future climates. Currently, climate models are only run on a few projected emissions scenarios, limiting decision makers' abilities to see the effects of potential decisions on climate mitigation without waiting months and spending millions of dollars in running the full simulations. The emulators produce in microseconds maps of the impacts of these choices on precipitation, temperature, and other important climate variables for decision makers working on climate mitigation. A version of this reduced climate model is al-

ready able to produce these maps and model a wide variety of policy changes in real time. For the success of the climate project, the creation of practical, easy-to-use tools and actionable predictions from scientific advancements are just as crucial scalable developments as engineering advances.

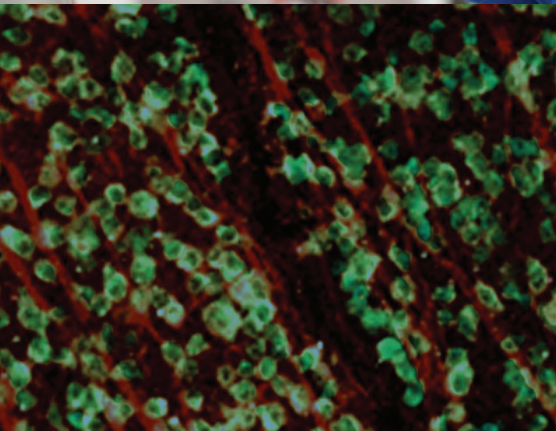
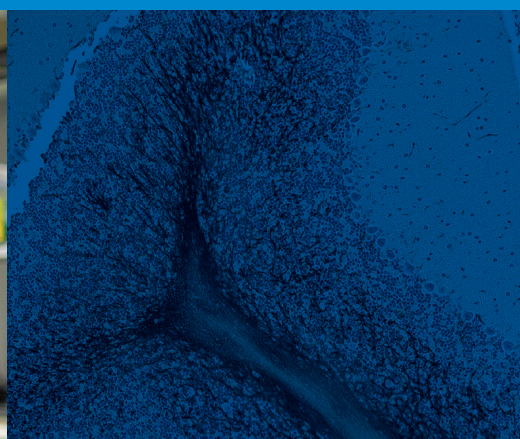
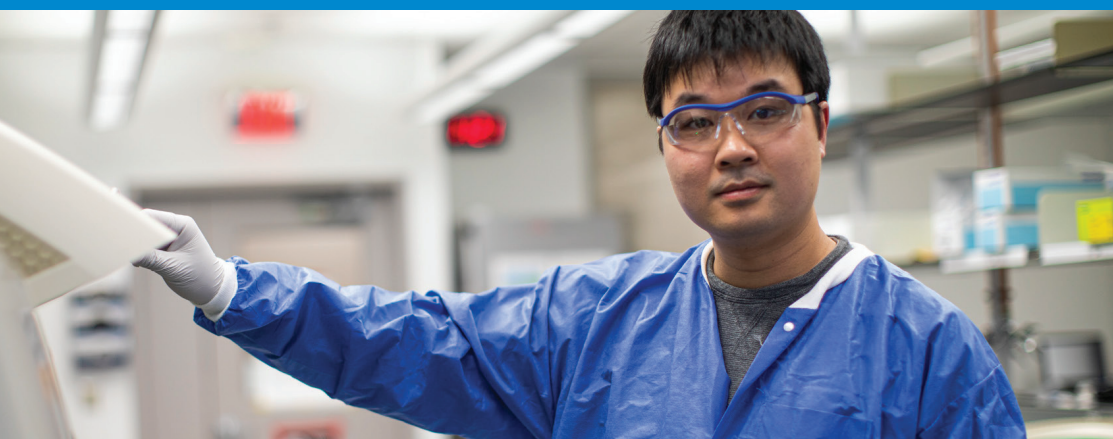
Another key emphasis of climate research is a focus on technologies to help with climate mitigation and adaptation for more vulnerable communities. Professor Elfatih Eltahir's work, in the Civil and Environmental Engineering Department, exemplifies this focus, especially his efforts on the Climate Resilience Early Warning System (CREWS-net). That project focuses specifically on climate adaptation in the southwestern region of Bangladesh, where there is a confluence of high natural risk from heat waves, cyclones, sea level rise, and land subsidence, and a large relatively poor agrarian population of 33 million. His work combines both scientific and engineering aspects, working on modeling to predict future climate risks and designing engineered solutions to address them. On the scientific side, his work uses high-resolution regional climate models to describe conditions such as precipitation, temperature, and sea level rise in a small region over a 30 year timespan. Then, these predictions are used in order to devise evidence and data driven engineering solutions that meet a variety of needs.

Broadly, Professor Eltahir is focusing on solutions to three broad classes of problems, namely those related to shelters, agriculture, and water security. For shelters, he is working on "adaptation fortresses" that are designed to provide protection from the wide range of potential weather disasters that can be induced by climate change, and provide the





# where science meets humanity™



## Innovation inspired by the passion of our people

As pioneers in neuroscience, Biogen discovers, develops and delivers worldwide innovative therapies for people living with serious neurological diseases as well as related therapeutic adjacencies. We are focused on advancing the industry's most diversified pipeline in neuroscience that will transform the standard of care for patients in several areas of high unmet need.

[biogen.com](http://biogen.com)



poor with access to clean drinking water. Similar “adaptation clinics” will provide knowledge and resources for farmers to adjust to the effects of climate change. Lastly, small-scale plants using reverse osmosis, set up with help from entrepreneurs, will help ensure water security. This work is being done in partnership with the large non-governmental organization BRAC, a Bangladesh-based international development group, which ensures that these solutions meet the needs of the affected populations. That partnership is also key to Professor Eltahir’s larger goal, which is to “lay the foundation” for development banks and agencies to develop further systems and infrastructure to help vulnerable populations everywhere adapt to climate change.

Overall, the MIT Climate Project helps unify and catalyze the wide range of climate research being done at MIT, with an especial emphasis on focusing on shepherding research and innovation from an academic setting towards making real advancements in technology, policy, and climate justice and mitigation. Beyond these goals, the Climate Project provides a great opportunity for members of the MIT community, especially undergraduates, to get involved with climate research at MIT and make a difference before even graduating college. All three professors emphasize the opportunities for students to get involved in the project, in ways ranging from conducting UROPs in climate, regardless of your major, to attending informational events on climate change, even to spearheading research projects of their own. Most importantly, it reflects the ability of an institution like MIT to focus its resources and create real, meaningful change in the world, and reminds its community of the potential it has to use science and engineering to improve the lives of all.



A decade of experience in transforming processes from batch to continuous

**CONTINUOUS**<sup>TM</sup>  
pharmaceuticals

[continuuspharma.com](http://continuuspharma.com) [info@continuuspharma.com](mailto:info@continuuspharma.com)

# MURJ Features

# Humanizing Science: In Conversation with Professor David Kaiser

FEATURING MIT PROFESSOR DAVID KAISER

By Charlotte Myers

The border between science and society is often drawn with bold, dramatic strokes—evoking images of mushroom clouds, moon landings, and mythic clashes between visionary scientists. While this framing holds undeniable allure, a more nuanced lens reveals a quieter, subtler story beneath these headlines, one that encompasses the many intricate ways that science and society are intertwined. Through this lens, science emerges not just as an institution in dramatic tension with society, but as a living, evolving reflection of it—complete with its own history, artistic expressions, and ethical dimensions that resonate with the culture that surrounds it.

Studying the history of science in its own right—not just at its dramatic intersections with world events—offers a unique lens for appreciating these often-overlooked dimensions. David Kaiser, Germeshausen Professor of the History of Science and Professor of Physics at MIT, is interested in exploring the history of science through this perspective. He emphasizes the importance of understanding the social institutions and dynamics that influence scientific progress at every level—from what questions are asked in the first place, to what problems are funded, to what ultimately emerges as a winning answer. Even the most singular scientific insights emerged “not only from the minds of influential thinkers,” Kaiser argues, but from a whirl of social forces: “shifting educational systems on the prerogatives of world wars, of the rise of fascism, of horrible inequities that we haven’t done nearly enough to try to get around in the scientific community.” An awareness about these historical factors is crucial for navigating the present landscape

of science. While it’s impossible to remove ourselves from the trends and pressures of the moment, Kaiser suggests that a historical perspective can help us to remain more mindful about our motivations: “Why am I chasing these questions? Because that’s a fad that’s going to vanish tomorrow, or because this has somehow grabbed a large number of us for reasons that might persist?”

This appreciation for the complexities in the history of science not only fosters mindfulness, but can offer a deeply humanizing perspective. While many are captivated by tales of scientific titans and the epic clashes between them, these tales can easily veer into myth, creating a divide between the legendary scientists of the past and the practitioners of the present. A closer look at the history of science, however, shatters that mythologization. In exploring the complex historical realities of science, we begin to see breakthroughs not merely as transcendent insights from supernatural figures, but as products inevitably shaped by historical and social factors. “The whole point should be that these are real people struggling to find answers to deep questions in real settings,” Kaiser emphasizes, suggesting that this humanizing approach is essential to avoid making “physics or physicists seem beyond reach.” This humanization is especially relevant with the resurgence of public interest in figures like Oppenheimer, exposing our tendency to both idolize and demonize scientists. A nuanced understanding of their historical context is crucial: “As long as we don’t make them into heroes or villains, then I think we’re hopefully leaving room open for extended discussion,” Kaiser argues.

Humanizing the history of science can have a deeply humbling effect on our perspective towards the present. While the history of science is marked by its great triumphs and deep failures, a closer look reveals the true fate of most ideas: a quiet fade into irrelevance. “Most of what gets published today in the scientific journals will not be shown to be wrong so much as just simply irrelevant, not so long from now,” Kaiser explains, a reality made undeniable by examining the quieter currents of scientific history. But rather than a cause for disillusionment, this reality can be reframed as liberating, freeing ourselves to focus not on producing definitive answers but on engaging authentically with the questions. “It helps me have a kind of sense of perspective that what we can do is try to advance the questions,” Kaiser reflects. “Our best attempt to answer those questions today might not be the last word, but we can try to refine and hone our questions, refine the toolkit, conceptual or sometimes literal tools, to try to get better at answering those questions- but not fool ourselves that our favorite answer today will be what everyone loves tomorrow.”

A nuanced historical study brings to light another often-overlooked dimension of science: the artistic. While science aims to objectively describe reality, it relies heavily on representations and visual tools to communicate its ideas. These visual tools are inherently artistic, aiming to distill and communicate complex scientific ideas just as a portrait aims to capture the essence of its subject. A prime example is the Feynman diagram, which, in an echo of other minimalist art forms, captures the vast complexity of particle interactions through a series of elegant lines and loops. Kaiser dissects this tool in “Drawing Theories Apart: The Dispersion of Feynman Diagrams in Postwar Physics,” examining how these diagrams emerged and took on a life beyond their initial purpose. In exploring this history, Kaiser found himself engaging with the “same questions art historians have been asking for generations: why do certain types of styles or artistic forms persist? Why

do they come to seem natural, or even inevitable, while others might seem so unusual or strange upon first seeing them?” But understanding the persistence of these visual forms also forces us to ask deeper questions about the training and social contexts that nurture them: Who is being trained, how do they learn, and what social forces shape their work? The persistence of Feynman diagrams, Kaiser argues, was not merely a result of mathematical utility, or even aesthetic appeal, but also of these social networks that spread them.

These artistic dimensions extend beyond the visual. Beyond its diagrams and data, science relies on storytelling to translate its discoveries, transforming technical findings into narratives that resonate with both experts and the broader world. Crafting metaphors and analogies to capture the essence of complex ideas is not merely a matter of technical accuracy, but of creative storytelling – an art form that often forces scientists to clarify and sharpen their own understanding. “I actually find it a great challenge to myself,” Kaiser shares. “Did I understand what I think I just did well enough to find the metaphors, the analogies, the little story or anecdote that can get some people who aren't paid to work on this all day to nonetheless pause and hopefully find that interesting as well.” But this communication is not just a trivial exercise – it is a public debt that scientists owe to the society which funds their research. “I think more of us hopefully will continue to do because so much of the work that we value today ultimately is paid for by taxpayers in the United States and elsewhere,” Kaiser argues.

But science’s duty to society doesn’t end at public outreach—it extends deeply into the ethical foundations of the field itself. Just as a historical study of science goes beyond its most dramatic moments, it is equally essential to recognize the subtle ways in which ethics is interwoven into the daily realities of scientific practice. For Prof. Kaiser, this complex reality should be reflected in our approach to scientific

*“Why am I chasing these questions? Because that's a fad that's going to vanish tomorrow, or because this has somehow grabbed a large number of us for reasons that might persist?”*



*"Manhattan Project." Accessed 24 November 2024. <https://www.nps.gov/mapr/oak-ridge.htm>*

education. At MIT, he and Prof. Julie Shah co-lead the Social and Ethical Responsibilities of Computing (SERC) initiative, aiming to embed ethical reflection into a series of classes, rather than relegating it to specialty courses. Their goal is to prepare students for the reality of ethical practice in science—not only as a consideration reserved for monumental, high-stakes decisions, but as an inevitable dimension in the routine choices of scientists.

A nuanced study of scientific history provides a more realistic picture of the mutual influence between science and society, revealing that they evolve together in a dynamic, symbiotic relationship that extends far beyond the dramatic moments of spectacle. Viewed through this lens, science emerges as a social institution in its own right—one that possesses not only its own history, but also distinct cultural and artistic forms that frame and communicate our understanding of the world, alongside ethical dimensions that guide our actions within it. Thus, the effort of humanizing science is not about merely adding a human element to a separate endeavor; it becomes a recognition of science as a deeply human practice.

# Turning the Tide: Combining Nanoparticles and Immunotherapy to Fight Pancreatic Cancer

By Cindy (Subin) Pyo

Pancreatic cancer, a cancer with only a five-year relative survival rate of 13%, has been on many scientists' and physicians' agenda for past decades (Hirshberg Foundation, 2024). In 2024, about 66,440 Americans were diagnosed with pancreatic cancer, and more than 51,570 were expected to die from the disease (Hirshberg Foundation, 2024).

Despite continued efforts by cancer researchers and advocates, pancreatic cancer has been difficult to treat and prevent due to several technical challenges. Because no markers or screening program have been identified, early detection is nearly impossible (Oberstein & Olive, 2013). As a result, when a patient is diagnosed, it is often at a time when surgical resection is unfeasible. Furthermore, pancreatic tumor is characterized by its aggressive nature and extensive heterogeneity of genetic mutations, thus possessing multiple levels of therapeutic resistance (Oberstein & Olive, 2013; Sarantis et al., 2020). In fact, the fibrotic or scar-like tissue around the tumor limits blood flow and immune cell access, contributing to chemotherapeutics and other kinds of drug delivery to fail (Ho et al., 2020). Consequently, chemotherapy and radiation have limited efficacy and have shown little to no success when applied in treatment.

While the prospect of pancreatic cancer treatment seems daunting, a recent discovery by a group of researchers at University of Massachusetts Chan Medical School opens an innovative pathway towards treating pancreatic cancer. Marcus Ruscetti, PhD, and Prabhani Atukorale, PhD, lead their team in creating a combined strategy of tackling the challenges of pancreatic cancer treatment: a cutting-edge combination therapy approach using nanoparticles (Fessenden, 2024).

The combined strategy comprises of a nanoparticle attached with two components: (1) immune-stimulating agents stimulator of interferon genes (STING) and Toll-like receptor 4 (TLR4), which wakes the host's immune system to fight cancer cells, and (2) protein kinase kinase (MEK) inhibitor trametinib and CDK4/6 inhibitor palbociclib, which suppress immune evading ability of tumor cells (Chibaya et al., 2024). This approach helps the treatment pass through the immune barrier more effectively. Given that one of the main challenges of drug delivery for pancreatic cancer patients is difficulty in immune infiltration, Dr. Ruscetti finds the dual therapy approach as a promising "strategy to get to the cancer cells and fight them" (Fessenden, 2024). Dr. Atukorale explains the novelty of the discovery: "we're attempting to build a 'smart therapy,' if you will. Just like your smartphone" (Saperstone, 2024).

Dr. Atukorale had previously discovered that treatment using nanoparticles co-loaded with immuno-agents on triple-negative breast cancer diagnosed mice resulted in significantly improved therapeutic outcomes (Atukorale et al., 2019). Based on these findings, the research team engineered a lipid-based nanoparticle that is biocompatible and able to encapsulate two immune-molecules that would activate the interferon genes pathway, which would allow the host's immune system to recognize the tumor cells as a threat (Fessenden, 2024). In addition, the researchers modified the nanoparticles to be lipid-based to ensure that it is able to penetrate through dense tumor microenvironments. Lipid-based nanoparticles offer several advantages for studies aimed on drug delivery into the tumor microenvironment: (1) they are more flexible and adaptable than rigid particles,

(2) as natural biological components, they are more biocompatible and less likely to trigger immune rejection, (3) the surface of lipid-based particles can be easily modified, which enhances their ability to bind to and penetrate specific types of immune-cells (Zhao et al., 2024).

The research team found promising results when they treated the lipid-based nanoparticles on pancreatic cancer mouse models. Firstly, they discovered that treatment led to increased uptake of

*"This innovative research highlights a promising new direction in the fight against pancreatic cancer, suggesting that combination therapy could significantly enhance patient outcomes."*

the nanoparticles by various immune and tumor cells. This triggered a strong immune response, including increased signaling from Type I interferon (signaling molecule), better presentation of tumor markers to the immune system, and activation of both innate (immediate) and adaptive (long-term) immune responses (Chibaya et al., 2024). Most importantly, the researchers found that dual treatment strategy resulted in significant tumor shrinkage and longer survival in the mice (Chibaya et al., 2024).

Previous results show that signaling induced by immune-stimulants STING and TLR4 is linked to improved immune responses in human pancreatic cancer cells (Chibaya et al., 2024). This study provides a feasible way to induce this signaling pathway in patients, raising the therapeutic possibility. Dr. Ruscetti affirms the treatment's human implications: "we envision that this could work in patients with very late stage tumors that unfortunately haven't responded to chemotherapy, other types of therapies as a way to activate the immune system to come in and target this cancer" (Saperstone, 2024). As the team continues their research, their goal is to "eventually take what [they're] doing in mice" into

the real world with hope of "really changing people's lives" (Saperstone, 2024). This innovative research highlights a promising new direction in the fight against pancreatic cancer, suggesting that combination therapy could significantly enhance patient outcomes. As the research team moves forward, they aim to transform their findings into effective treatments that offer hope to those battling this aggressive disease.

## References

[1] Atukorale, P. U., Raghunathan, S. P., Raguveer, V., Moon, T. J., Zheng, C., Bielecki, P. A., Wiese, M. L., Goldberg, A. L., Covarrubias, G., Hoimes, C. J., & Karathanasis, E. (2019). Nanoparticle encapsulation of synergistic immune agonists enables systemic codelivery to tumor sites and ifn $\beta$ -driven antitumor immunity. *Cancer Research*, 79(20), 5394–5406. <https://doi.org/10.1158/0008-5472.can-19-0381>

[2] Chibaya, L., DeMarco, K. D., Lusi, C. F., Kane, G. I., Brassil, M. L., Parikh, C. N., Murphy, K. C., Chowdhury, S. R., Li, J., Ma, B., Naylor, T. E., Cerrutti, J., Mori, H., Diaz-Infante, M., Peura, J., Pitarresi, J. R., Zhu, L. J., Fitzgerald, K. A., Atukorale, P. U., & Ruscetti, M. (2024). Nanoparticle delivery of innate immune agonists combined with senescence-inducing agents promotes T cell control of pancreatic cancer. *Science Translational Medicine*, 16(762). <https://doi.org/10.1126/scitranslmed.adj9366>

[3] Fessenden, J. (2024, September 4). UMass Chan researchers develop dual therapeutic that holds promise as pancreatic cancer treatment. UMass Chan Medical School. <https://www.umassmed.edu/news/news-archives/2024/09/umass-chan-researchers-develop-dual-therapeutic-that-holds-promise-as-pancreatic-cancer-treatment/>

[4] Ho, W. J., Jaffee, E. M., & Zheng, L. (2020). The tumour microenvironment in pancreatic cancer — clinical challenges and opportunities. *Nature Reviews Clinical Oncology*, 17(9), 527–540. <https://doi.org/10.1038/s41571-020-0363-5>

[5] Oberstein, P. E., & Olive, K. P. (2013). Pancreatic cancer: shy is it so hard to treat? *Therapeutic Advances in Gastroenterology*, 6(4), 321–337. <https://doi.org/10.1177/1756283x13478680>

Pancreatic Cancer Facts. Hirshberg Foundation



for Pancreatic Cancer Research. (2024, January 31). <https://pancreatic.org/pancreatic-cancer/pancreatic-cancer-facts/#:~:text=to%20earlier%20diagnosis.-,Pancreatic%20cancer%20has%20the%20highest%20mortality%20rate%20of%20all%20major,survival%20rate%20is%20only%2044%25>

[6] Saperstone, J. (2024, September 20). New cancer research breakthrough has the potential to save lives. NBC Boston. <https://www.nbcboston.com/news/local/new-cancer-research-has-the-potential-to-save-lives/3494882/>

[7] Sarantis, P., Koustas, E., Papadimitropoulou, A., Papavassiliou, A. G., & Karamouzis, M. V. (2020). Pancreatic ductal adenocarcinoma: Treatment hurdles, tumor microenvironment and immunotherapy. *World Journal of Gastrointestinal Oncology*, 12(2), 173–181. <https://doi.org/10.4251/wjgo.v12.i2.173>

[8] Zhao, C., Zhu, X., Tan, J., Mei, C., Cai, X., & Kong, F. (2024). Lipid-based nanoparticles to address the limitations of GBM therapy by overcoming the blood-brain barrier, targeting glioblastoma stem cells, and counteracting the immunosuppressive tumor microenvironment. *Biomedicine & Pharmacotherapy*, 171, 116113. <https://doi.org/10.1016/j.biopha.2023.116113>

# MURJ Spotlights

## RESEARCH SPOTLIGHT

## Esme Sun

MIT Class of 2025

Computer Science and Molecular Biology

Since her sophomore year of high school, Esme Sun has been drawn to gene editing technologies. Inspired by the biological ingenuity of CRISPR-based tools, which allow scientists to modify cellular DNA, Esme directed her first research project at just 15 years old; she used a CRISPR-based epigenetic tool to target and activate a gene implicated in depression.

Now, six years later, Esme is developing her own CRISPR-based epigenetic tool and is on a mission to advance understanding of critical epigenetic pathways and broaden the possibilities for gene therapy to tackle diseases that were once considered untreatable.

Esme's research journey at MIT began in Professor George Church's Lab at the Wyss Institute for Biologically Inspired Engineering. There, Esme spent her freshman summer working on pioneering delivery technology in genetic medicine. "Gene therapy is incredibly promising, but actually getting the therapy to the right place in the body for it to be effective is currently a huge challenge," Esme explained. "I was studying the possibilities of using different viral proteins to infect and deliver genes to intended cells." During her spotlight interview, Esme also discussed her experience joining a large lab. "The Church Lab was always busy, and there were dozens of researchers working on a multitude of different projects," Esme said. "That aspect of research was new to me, and it took me a while to adapt to being in such a big lab, but I really enjoyed the opportunity to learn about all the cool things people there were working on."

A year later, Esme decided to explore the field of gene editing more directly by spearheading a new project: build-

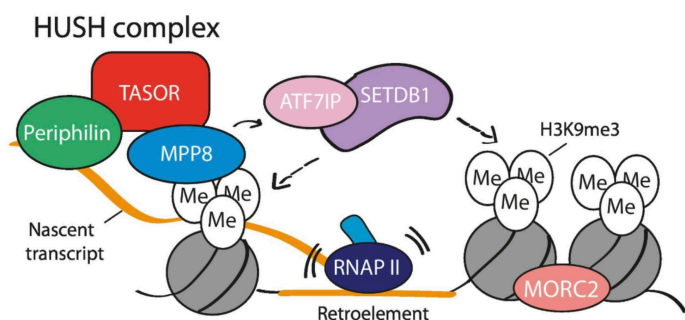


Fig. 1. Human silencing hub (HUSH) – a complex of transcription activation suppressor (TASOR), M-phase phosphoprotein 8 (MPP8), and periphilin – is an epigenetic repressor that promotes deposition of histone 3 lysine 9 trimethylation (H3K9me3).



ing a novel epigenetic silencing tool at Professor Jonathan Weissman's Lab at the Whitehead Institute for Biomedical Research. Epigenetics is the study of how gene activity is regulated without altering the underlying DNA sequence. This field is particularly important in medicine, as disruptions in epigenetic processes are linked to numerous diseases, including cancer and neurological disorders. "I'm currently engineering a CRISPR-based tool that utilizes the HUSH complex, a human protein complex with the ability to silence dangerous genetic elements using epigenetic modifications," Esme said (Figure 1). "By using a tool I built to study this [complex], we have been able to discover more about its endogenous silencing mechanisms and are currently working to improve and adapt this tool to continue to expand our knowledge of epigenetic silencing."

Equipped with her experiences working on gene editing research, Esme is excited to continue her research journey in graduate school, aiming to uncover novel insights about the molecular dynamics of, and potential treatments for, neurological and psychiatric diseases. "There's so much potential [in studying epigenetics and gene-editing] that I haven't explored yet," Esme said. "I'm excited to see where my research goes next."

## References

Seczynska, M., Bloor, S., Cuesta, S. M., & Lehner, P. J. (2022). Genome surveillance by HUSH-mediated silencing of intronless mobile elements. *Nature*, 601(7893), 440–445. <https://doi.org/10.1038/s41586-021-04228-1>

## RESEARCH SPOTLIGHT

# Victory Yinka-Banjo

MIT Class of 2025

Computer Science and Molecular Biology

*“Biology and computer science became the subjects I couldn’t stop thinking about, even sometimes falling asleep imagining the ways in which they could overlap.”*

Victory Yinka-Banjo is determined to “approach biological problems through different lenses—whether manipulating cells in the lab or analyzing them with advanced algorithms.” Her research experience has reinforced her goal and passion for helping bridge the gap between computation and the life sciences to derive biologically meaningful insights that could impact human health.

At the Weissman Lab, Victory helped work with a team exploring a natural gene silencing tool called the HUSH protein complex to artificially silence genes, which allowed her to work directly with biological samples—designing and expressing proteins in cell lines, and analyzing gene expression with flow cytometry. “This was critical in my research experience. It taught me how to troubleshoot in experimental design and how research can be directly tied to medical applications beyond the lab.”

After working in the wet lab, Victory was drawn to an ongoing intensive dry lab project. It gave her the opportunity to integrate her skills and interests in computational sciences and biology. “My next project has involved 15 months of working with deep learning architectures at the Uhler Lab,” she shares. Victory’s intensive endeavor leveraged computational tools to analyze biological data. At the Uhler Lab at the Broad Institute of MIT and Harvard, she is studying how polygenic risk scores for metabolic diseases impact the structure of fat cells. “This experience has strengthened my skills in data analysis and evaluating findings to determine their biological relevance. It also made me even more excited about cell biology, molecules, and the environments in which they operate.” At present, that love has led Victory to apply to grad school for molecular studies. “It’s an exciting time in this area of research! The 2024 Nobel Prize awardees used AI models to predict complex protein structures and design new proteins—the possibilities in research inspire me, and I hope to inspire people with the work I do.”

Victory is clear and purposeful in her ambitions. “Cli-



ché, but I do want to help change the world in some way,” she began, “and I will. But, the world starts for me in Nigeria.” Victory is President of the African Students’ Association (ASA), a former leader on the MIT Biotechnology Group’s (MBG) executive team, and an avid researcher, all the while balancing and excelling in her academic and social life at MIT. Victory is working to make an impact back home, pursue computational biology in her grad studies and beyond, and embark on a life-long journey of improving human health with her work.

# MURJ

# UROP

# Summaries

# Mapping Mindfulness: A Systematic Review of the Neuroanatomy Associated with Mindfulness

Kannammai Pichappan<sup>1</sup>, Isaac Treves<sup>2</sup>, John Gabrieli<sup>3</sup>

<sup>1</sup> Student Contributor, Class of 2026, Department of Brain & Cognitive Sciences, MIT, Cambridge, MA, 02139

<sup>2</sup> Supervisor, Department of Brain & Cognitive Sciences, MIT, Cambridge, MA, 02139

<sup>3</sup> Principal Investigator, Department of Brain & Cognitive Sciences, MIT, Cambridge, MA, 02139

## Introduction

Mindfulness is the psychological process of bringing one's attention to experiences occurring in the present moment. This research explores how mindfulness influences brain structure and, consequently, mental well-being. We identify four core mechanisms through which mindfulness operates: emotion regulation, body awareness, self-awareness, and attention.

## Methods

The studies examined here utilized various neuroimaging techniques to assess structural changes in the brain across different populations, including those with high dispositional mindfulness (DM; the natural ability to focus on and sustain attention to present-moment experiences with openness and without judgment), long-term meditators (LTM), and individuals undergoing mindfulness interventions. We employed a rigorous methodology (Figure 1) to select papers for consideration.

## Results

The findings are organized according to the four core mechanisms of mindfulness:

### Emotion Regulation (Figure 2)

1. **Amygdala:** Smaller amygdala sizes (by volume) were associated with increased DM, potentially explaining reduced stress reactivity in more mindful individuals. This finding is meaningful as the amygdala plays a key role in processing emotions—especially fear—and increased amygdala volume is linked to a higher risk of stress-related pathologies. (Lu, 2014; Taren, 2013; Murakami 2012).
2. **Right Hippocampus:** Increased volume in the right hippocampus—involved in spatial memory, emotional regulation, and long-term memory—was observed with increased DM, consistent with findings from LTM and intervention studies. This change was reported in multiple studies (Luders, 2009; Hölzel, 2008; Kang, 2013; Hölzel, 2011; Pickut, 2013; Wells, 2013).
3. **Anterior Cingulate Cortex (ACC) and Corona Radiata:** Both the volume and fractional anisotropy (a measure in brain imaging that shows the level of directionality of water movement, with higher values generally indicating more organized tissue) of these brain regions increased with DM, respectively. The increased gray matter volume in

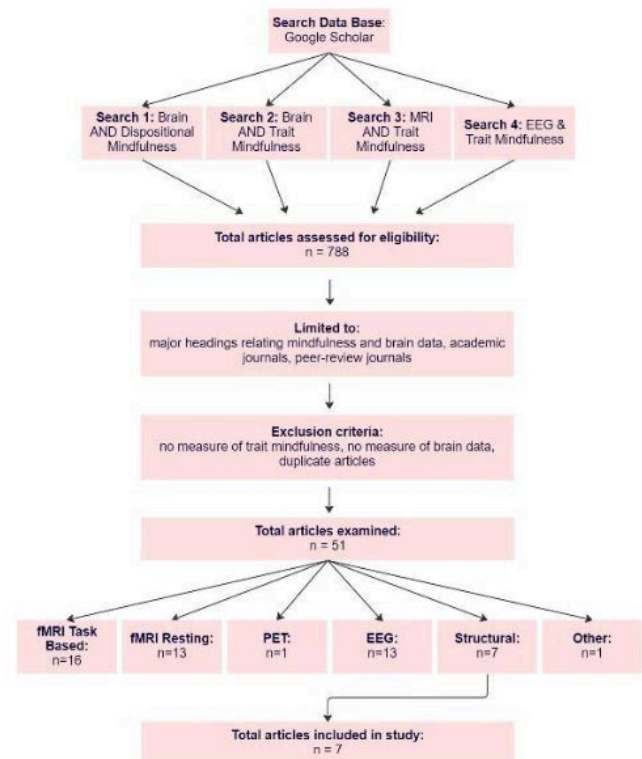


Fig. 1. Flow chart illustrating systematic study selection process.

the ACC, which supports cognitive control and decision-making, could be attributed to enhanced communication efficiency in the corona radiata, a key region in processing sensory and motor information. (Lu, 2014; Boekel, 2018).

4. **Prefrontal Cortex (PFC):** As DM increased, there was an observed increase in the surface area of the PFC, a region involved in executive functions. This observation aligns with fMRI studies, which have shown that increased DM correlates with higher degrees of activation in prefrontal regions involved in emotion regulation (Allen, 2012; Zeidan, 2014).
5. **Orbitofrontal Cortex (OFC):** Interestingly, the volume of the OFC—involved in emotion regulation tasks—decreased as DM increased, despite previous fMRI studies

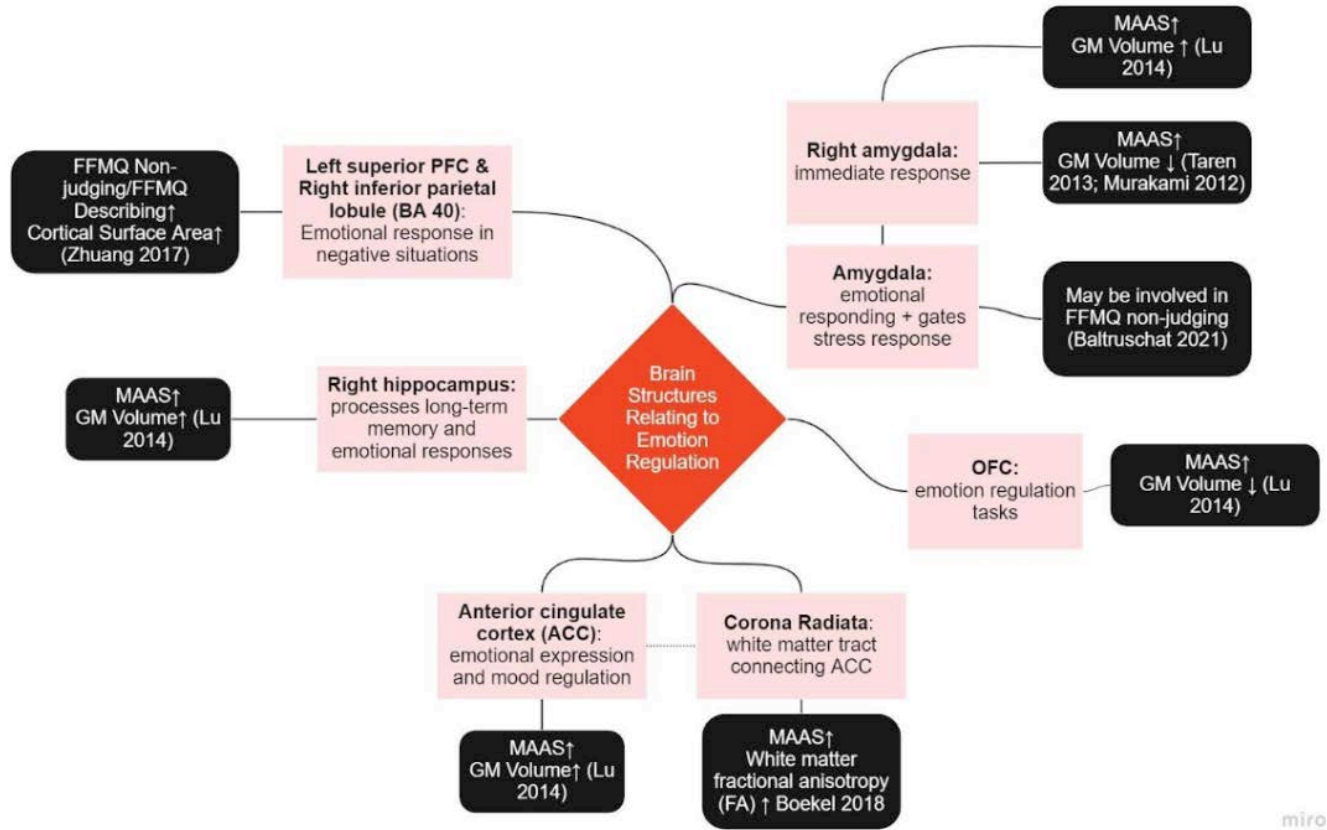


Fig. 2. Mindfulness bolsters mental function by altering brain structures relating to emotion regulation. MAAS = Mindful Attention Awareness Scale (a 15-item survey that measures a person's mindfulness); FFMQ = Five Facet Mindfulness Questionnaire (a 39-item self-report survey that measures a person's mindfulness in five areas).

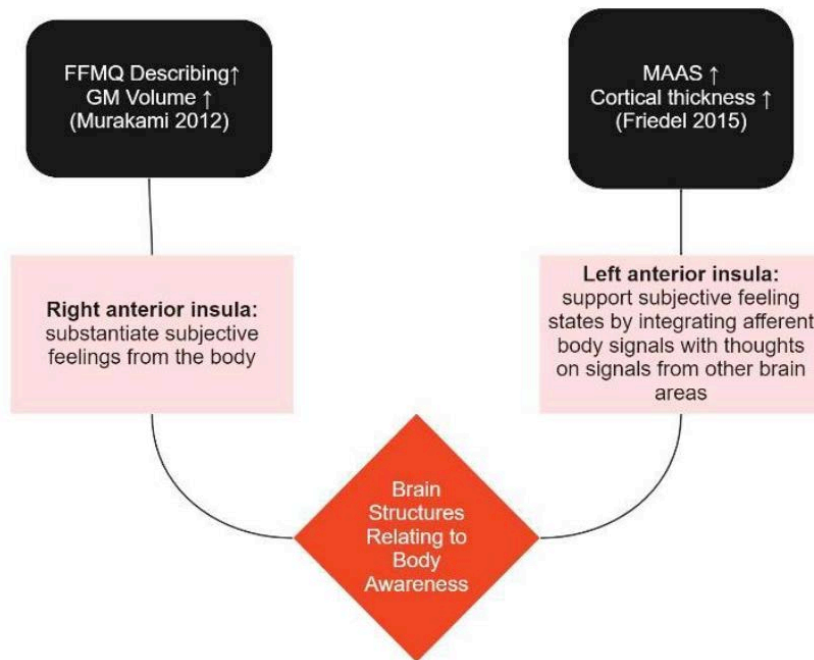


Fig. 3. Mindfulness bolsters mental function by altering brain structures relating to body awareness.

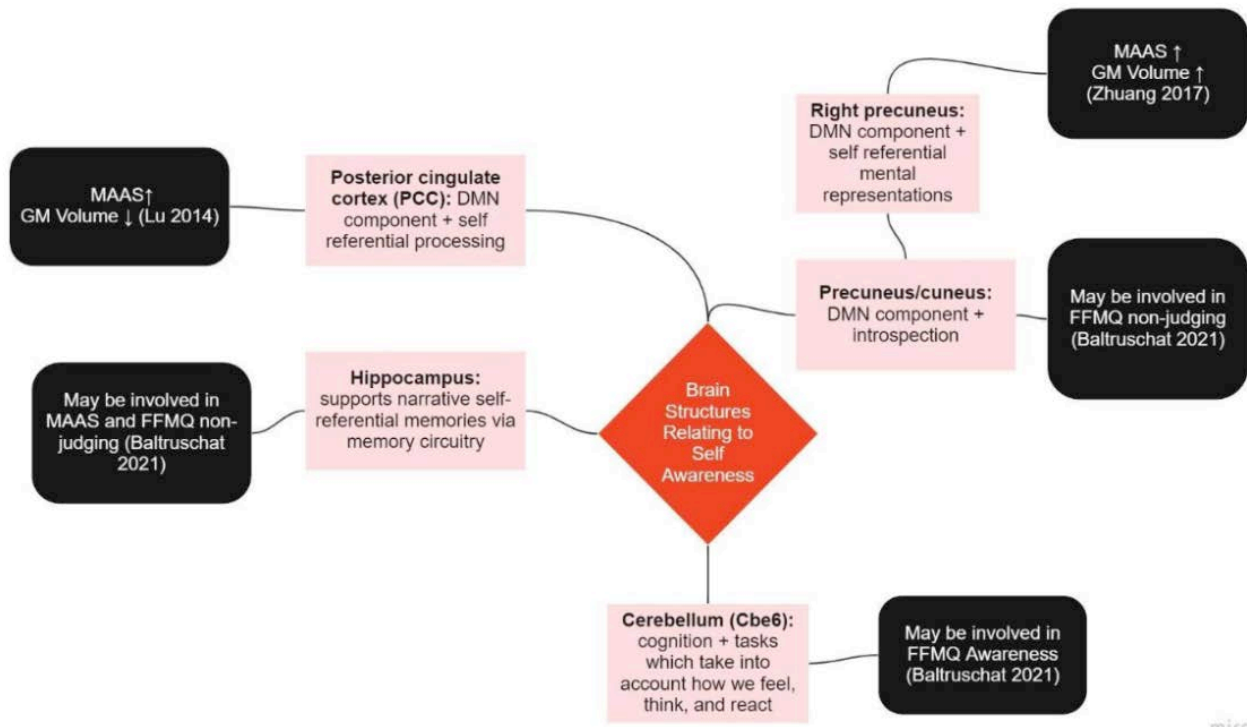


Fig. 4. Mindfulness bolsters mental function by altering brain structures relating to self-awareness.

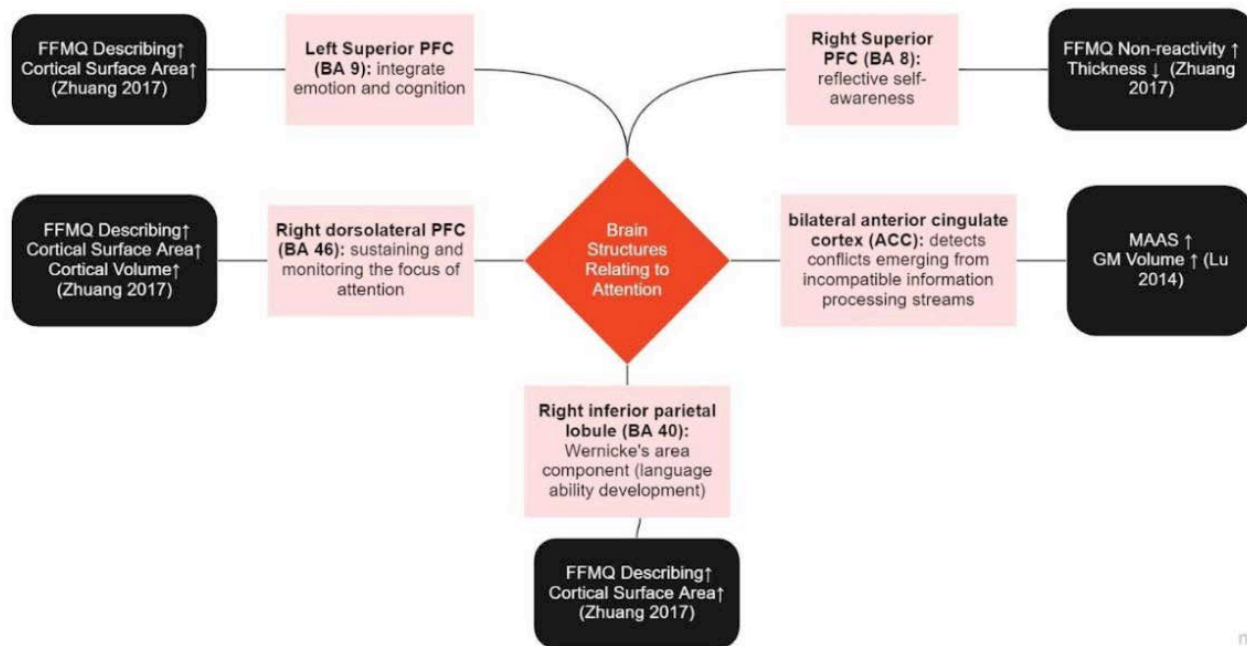


Fig. 5. Mindfulness bolsters mental function by altering brain structures relating to attention.



showing an association between higher levels of trait mindfulness and increased OFC activation (Kong, 2016).

#### **Body Awareness** (Figure 3)

1. **Left Anterior Insula:** The left anterior insula forms part of the insular cortex and is involved in functions like emotional awareness, empathy, and interoception. It plays a key role in integrating sensory and emotional information. Increased DM at age 19 was associated with decreased thinning of the cortical regions of the brain from ages 16 to 19, suggesting a protective effect during adolescent development (Friedel, 2015).
2. **Right Anterior Insula:** The right anterior insula is involved in substantiating subjective feelings from the body. Volume increases were observed with higher DM, consistent with findings from intervention and LTM studies (Hölzel, 2008; Lazar, 2005).

#### **Self-Awareness** (Figure 4)

1. **Hippocampus and Cerebellum:** The hippocampus supports narrative self-referential memories, and the cerebellum is involved in cognition and tasks that consider how we feel, think, and react. Structural changes associated with DM were observed in both regions. Increased gray matter volume was reported in LTM and intervention studies (Luders, 2009; Hölzel, 2011; Pickut, 2013).
2. **Posterior Cingulate Cortex (PCC):** The PCC is involved in self-referential processing. Its volume decreased as DM increased, indicating a reduced tendency for self-rumination – a negative and persistent pattern of thinking about oneself. (Lu, 2014).
3. **Right Precuneus:** Volume increased with DM, indicating enhanced self-awareness. (Zhang, 2017).

#### **Attention** (Figure 5)

1. **Prefrontal Cortex (PFC):** Increases in cortical surface area and volume were observed in the left superior PFC—responsible for integrating emotion and cognition—and right dorsolateral PFC—responsible for reflective self-awareness—with higher DM. Activation increases were also noted in intervention studies (Allen, 2012).
2. **Parietal Lobe:** The cortical surface area of the parietal lobe, which is responsible for processing and making sense of sensory information, increased with DM.
3. **Right Superior PFC:** Thickness decreased as DM increased, while volume increased in intervention studies (Hölzel et al., 2008; Lazar et al., 2005).
4. **ACC:** Volume increased with DM, consistent with findings from increased activity in intervention studies (Zeidan, 2014) and increased cortical thickness in LTM studies (Grant, 2010).

### **Discussion**

The results provide valuable insights into the mechanisms through which mindfulness works and the shared neural bases of mental illnesses. The structural changes associated with dispositional mindfulness might explain the link between mindfulness practices and positive mental health outcomes.

Potential applications of these findings include:

1. Investigating the presence and strength of associations between dispositional mindfulness and various mental health conditions, including depression, anxiety, suicidal ideation, and bipolar disorder
2. Administering mindfulness interventions for both diagnosed and at-risk individuals
3. Incorporating mindfulness practices into educational systems as a preventive measure
4. Using brain structures as potential biomarkers for mental illness risk

Some limitations of this study are the inconsistencies in neuroanatomy results among different studies and the limited literature specifically addressing DM and brain structure (only seven studies were available).

### **Conclusion**

This systematic review underscores the potential of mindfulness to foster mental well-being through alterations in brain structure. By elucidating the neural mechanisms underlying mindfulness practices, this research paves the way for future investigations into mindfulness as a therapeutic tool for enhancing mental health across diverse populations.

Our findings suggest that mindfulness practices can lead to structural changes in brain regions associated with emotion regulation, body awareness, self-awareness, and attention. These changes underlie the positive mental health outcomes observed in individuals with higher levels of dispositional mindfulness.

The study's comprehensive approach, combining insights from dispositional mindfulness, long-term meditator, and intervention studies, provides a robust foundation for understanding the neurobiological effects of mindfulness. This integrated perspective allows for a more nuanced understanding of how different aspects of mindfulness practice may contribute to brain plasticity, the brain's intrinsic ability to adapt and change at the structural and functional level, and mental well-being.

Future research directions include longitudinal studies to track brain changes over time with different mindfulness practices, investigations into the optimal duration and type of mindfulness interventions for specific outcomes, and exploration of potential synergies between mindfulness and other therapeutic approaches.

In conclusion, this research not only advances our understanding of the neural mechanisms underlying mindfulness but also highlights its potential as a powerful tool for promoting mental health and well-being. The findings suggest that integrating mindfulness practices into educational systems and clinical settings can be a proactive approach to mental health.

### **References**

- Allen, Michael. (2012). Cognitive-affective neural plasticity following active-controlled mindfulness intervention. *Journal of Neuroscience*, 32, 15601-15610. Retrieved on September 27, 2024 from <https://www.jneurosci.org/content/32/44/15601>
- Baltruschat, Sabina. (2021). There is more to mindfulness than emotion regulation: A study on brain structural networks. *Frontiers in Psychology*, 12. Retrieved on September 27, 2024 from <https://www.frontiersin.org/articles/10.3389/fpsyg.2021.659403/full>
- Bauer, Clemens C. (2019). Mindfulness training reduces stress and amygdala reactivity to fearful faces in middle-school children. *Behavioral Neuroscience*, 133, 569–585. Retrieved on September 27, 2024 from <https://psycnet.apa.org/record/2019-73636-001>

- Bauer, Clemens C. (2020). Mindfulness training preserves sustained attention and resting state anticorrelation between default-mode network and dorsolateral prefrontal cortex: A randomized controlled trial. *Human Brain Mapping*, 41, 5356–5369. Retrieved on September 27, 2024 from <https://onlinelibrary.wiley.com/doi/full/10.1002/hbm.25197>
- Boekel, Wouter. (2018). Cross-sectional white matter microstructure differences in age and trait mindfulness. *PLOS ONE*, 13. Retrieved on September 27, 2024 from <https://journals.plos.org/plosone/article?id=10.1371/journal.pone.0205718>
- Crego, Antonio. (2021). Relationships between mindfulness, purpose in life, happiness, anxiety, and depression: Testing a mediation model in a sample of women. *International Journal of Environmental Research and Public Health*, 18, 925. Retrieved on September 27, 2024 from <https://www.mdpi.com/1660-4601/18/3/925>
- Friedel, Susanne. (2015). Dispositional mindfulness is predicted by structural development of the insula during late adolescence. *Developmental Cognitive Neuroscience*, 14, 62–70. Retrieved on September 27, 2024 from <https://www.sciencedirect.com/science/article/pii/S1878929315000717>
- Grant, Joshua A. (2010). Cortical thickness and pain sensitivity in zen meditators. *Emotion*, 10, 43. Retrieved on September 27, 2024 from <https://psycnet.apa.org/record/2010-01983-005>
- Hölzel, Britta K. (2008). Investigation of mindfulness meditation practitioners with voxel-based morphometry. *Social Cognitive and Affective Neuroscience*, 3, 55–61. Retrieved on September 27, 2024 from <https://academic.oup.com/scan/article/3/1/55/1611219>
- Hölzel, Britta K. (2011). Mindfulness practice leads to increases in regional brain gray matter density. *Psychiatry Research: Neuroimaging*, 191, 36–43. Retrieved on September 27, 2024 from <https://www.sciencedirect.com/science/article/abs/pii/S092549271000288X>
- Jones, Payton. (2019). Mindfulness training: Can it create superheroes?. *Frontiers in Psychology*, 10, 613. Retrieved on September 27, 2024 from <https://www.frontiersin.org/articles/10.3389/fpsyg.2019.00613/full>
- Lazar, Sara W. (2005). Meditation experience is associated with increased cortical thickness. *Neuroreport*, 16, 1893. Retrieved on September 27, 2024 from [https://journals.lww.com/neuroreport/Abstract/2005/11280/Meditation\\_experience\\_is\\_associated\\_with\\_increased.5.aspx](https://journals.lww.com/neuroreport/Abstract/2005/11280/Meditation_experience_is_associated_with_increased.5.aspx)
- Kang, Yoona. (2013). Mindfulness and de-automatization. *Emotion Review*, 5, 192–201. Retrieved on September 27, 2024 from <https://journals.sagepub.com/doi/10.1177/1754073912451629>
- Kong, Feng. (2016). Brain regions involved in dispositional mindfulness during resting state and their relation with well-being. *Social Neuroscience*, 11, 331–343. Retrieved on September 27, 2024 from <https://www.tandfonline.com/doi/abs/10.1080/17470919.2015.1092469>
- Lu, Hongchao. (2014). The brain structure correlates of individual differences in trait mindfulness: A voxel-based morphometry study. *Neuroscience*, 272, 21–28. Retrieved on September 27, 2024 from <https://www.sciencedirect.com/science/article/abs/pii/S0306452214003431>
- Luders, Eileen. (2009). The underlying anatomical correlates of long-term meditation: larger hippocampal and frontal volumes of gray matter. *Neuroimage*, 45, 672–678. Retrieved on September 27, 2024 from <https://www.sciencedirect.com/science/article/abs/pii/S1053811909000044>
- Murakami, Hiroki. (2012). The Structure of Mindful Brain. *PLoS ONE*, 7. Retrieved on September 27, 2024 from <https://journals.plos.org/plosone/article?id=10.1371/journal.pone.0046377>
- Pickut, Barbara A. (2013). Mindfulness based intervention in Parkinson's disease leads to structural brain changes on MRI: a randomized controlled longitudinal trial. *Clinical Neurology and Neurosurgery*, 115, 2419–2425. Retrieved on September 27, 2024 from <https://www.sciencedirect.com/science/article/abs/pii/S0303846713002934>
- Taren, Adrienne A. (2013). Dispositional mindfulness co-varies with smaller amygdala and caudate volumes in community adults. *PLoS ONE*, 8. Retrieved on September 27, 2024 from <https://journals.plos.org/plosone/article?id=10.1371/journal.pone.0064574>
- Wells, Rebecca E. (2013). Meditation's impact on default mode network and hippocampus in mild cognitive impairment: a pilot study. *Neuroscience Letters*, 556, 15–19. Retrieved on September 27, 2024 from <https://www.sciencedirect.com/science/article/abs/pii/S0304394013009087>
- Zeidan, Fadel. (2014). Neural correlates of mindfulness meditation-related anxiety relief. *Social Cognitive and Affective Neuroscience*, 9, 751–759. Retrieved on September 27, 2024 from <https://academic.oup.com/scan/article/9/6/751/1664700>
- Zhuang, Kaixiang. (2017). A distinction between two instruments measuring dispositional mindfulness and the correlations between those measurements and the neuroanatomical structure. *Scientific Reports*, 7. Retrieved on September 27, 2024 from <https://www.nature.com/articles/s41598-017-06599-w>
- Zoogman, Sarah. (2014). Mindfulness interventions with youth: A meta-analysis. *Mindfulness*, 6, 290–302. Retrieved on September 27, 2024 from <https://link.springer.com/article/10.1007/s12671-013-0260-4>

# Empowering Student Wellbeing Through Technology: Insights from a Digital Phenotyping Study on Stress and Sleep Quality

Ariadne Dulchinos<sup>1</sup>, Edwin Ouko<sup>2</sup>, Sabrina Do<sup>2</sup>, Valerie Kwek<sup>2</sup>, Somaia Saba<sup>3</sup>, Richard Fletcher<sup>4</sup>

<sup>1</sup> Student Contributor, Class of 2025, Department of Computer Science and Cognitive Science, MIT, Cambridge, MA, 02139

<sup>2</sup> Student Contributor, Class of 2026, Department of Computer Science, MIT, Cambridge, MA, 02139

<sup>3</sup> Department of Computer Science, MIT, Cambridge, MA, 02139

<sup>4</sup> Principal Investigator, Department of Mechanical Engineering, MIT, Cambridge, MA, 02139

## Introduction

Recent studies have underscored the exacerbation of mental health challenges such as anxiety and depression among U.S. college students, particularly intensified by the COVID-19 pandemic (Roberts, 2023). This period highlighted the intricate link between academic pressures and mental health, revealing that students' stress directly correlates with their mental well-being and academic outcomes (Roberts, 2023). Further research into the sources of stress among college students illustrates a significant dose-response relationship, indicating that increased stress in various life domains escalates the risk of mental health disorders (Karyotaki, 2020). Moreover, sleep quality has emerged as a critical factor influencing learning and overall academic performance. Studies have shown that suboptimal sleep, especially prevalent among students during exam periods, significantly detracts from their academic success and health (Ez ElArab, 2014; Zeek, 2015). These findings underscore the necessity of adequate

sleep for maintaining academic performance and highlight sleep's role as a fundamental component of student health and well-being.

In light of these challenges, there is a compelling need for innovative approaches to monitoring and improving student well-being through real-time analysis of stress, sleep, and daily behaviors. Our study leverages digital phenotyping, a method that employs passive monitoring via smartphone sensors, to provide a nuanced understanding of these factors (Onnela, 2016; Oudin, 2023). Utilizing the MobilePath platform (Do, 2023), this study harnesses detailed behavioral data alongside proactive questionnaires to foster timely interventions that can significantly mitigate stress, enhance sleep quality, and ultimately boost academic performance. Our research represents a crucial step toward employing technology-driven solutions to optimize student well-being in challenging academic environments.

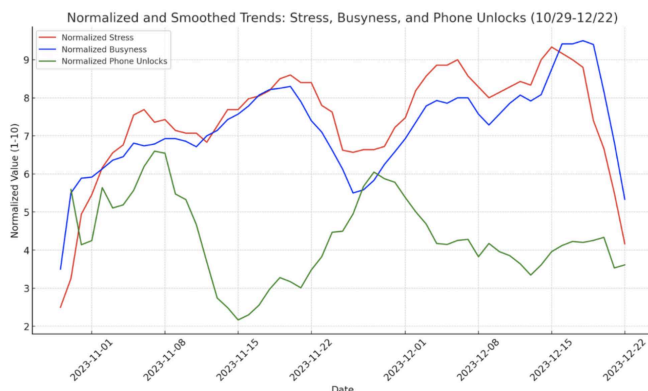


**Fig. 1. Trend Analysis of Stress, Busyness, and Phone Unlocks Over Time.** Trends of stress, busyness, and phone unlocks from October 29 to December 22 show a correlation between stress (red line) and busyness (blue line), indicating that busier days often have higher stress levels. However, phone usage (green line) displays a variable relationship and does not consistently follow the trends of stress and busyness. Notably, phone usage does not increase with peaks in stress and busyness during mid-November and early December, likely impacted by academic pressures such as midterms. Towards the end of December, as stress and busyness decline, possibly due to the holiday break, phone usage slightly rises, suggesting increased leisure time.

## Methods

This pilot study at MIT, conducted from October 29 to December 22, obtained 160 active questionnaire responses and collected daily passive monitoring data from students using the MobilePath platform. Ethical approval was secured from the MIT consent board, and data privacy was strictly maintained with encrypted data uploads to a secure server. Participants, all graduate students aged 18-28, provided written informed consent. Data collection was facilitated through smartphone sensors, including accelerometers, GPS, phone unlock events, and call/text logs. The baseline questionnaire included questions about sleep patterns and quality (e.g., typical sleep schedules for workdays and weekends and overall sleep quality ratings over the past month on a four-point scale) and sleep-related medication use. It also included mental health screening (e.g., the Generalized Anxiety Disorder-7 (GAD-7) for anxiety symptoms and the Patient Health Questionnaire-9 (PHQ-9) for depressive symptoms). Participants indicated significant academic deadlines (e.g., exams and projects). The daily questionnaire included questions about daily busyness and stress levels (e.g., participants rated the intensity of their day and stress levels on a ten-point scale), primary sources of stress, and sleep schedule disruptions.

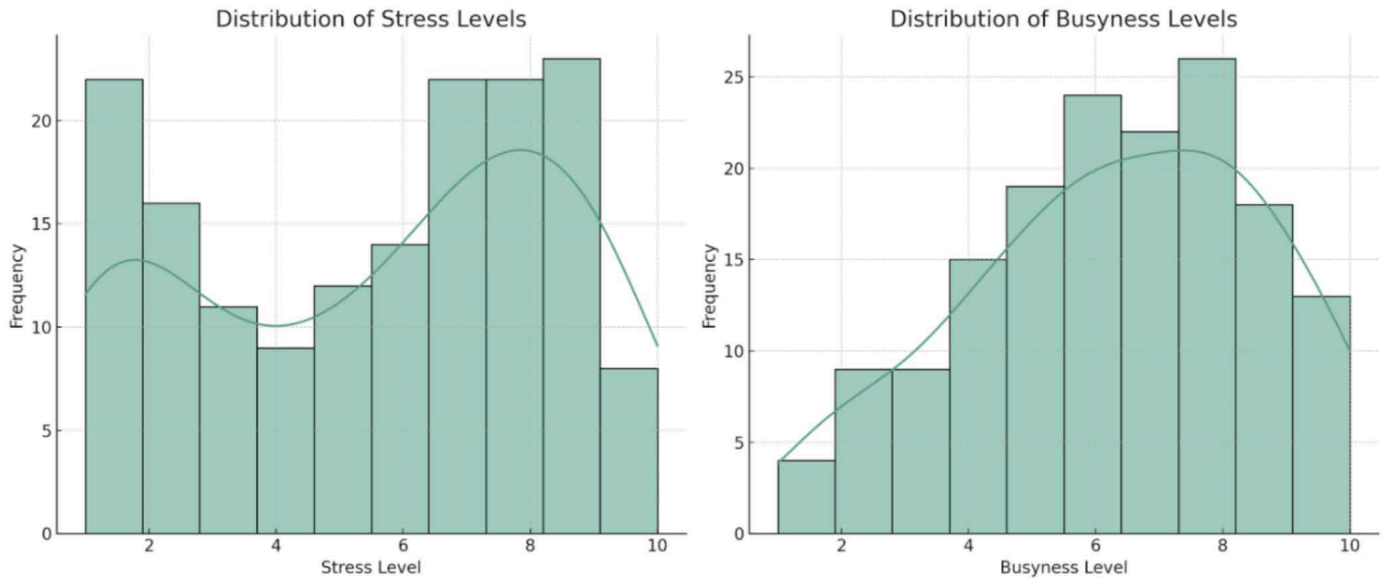


**Figure 2: Comparative Distribution of Stress and Busyness Levels Among Participants.** The daily stress levels reported by participants showed a bimodal distribution with peaks at 2 and 8, reflecting a range from moderate to high stress among respondents. This finding suggests significant stressors within the academic environment. Conversely, the daily busyness levels displayed an unimodal distribution peaking at 7, indicating that most students find their schedules demanding. The data points to times when high stress and busyness coincide, highlighting potential time management challenges in students’ academic lives. However, there are periods where high stress occurs without high busyness, suggesting other underlying stress factors.

**Results**

**Stress and Busyness:** Analysis illustrated a pattern where periods of high academic demand, such as midterms and project deadlines, led to increased stress and busyness levels among students. The data, as seen in Figure 1, showed that stress levels (red line) spiked concurrently with busyness (blue line), indicating a direct correlation between workload and stress. In contrast, phone unlocks, shown by the green line, do not consistently follow this trend; while phone usage slightly increases during the less busy holiday period at the end of December, it does not rise in conjunction with stress and busyness peaks. A bimodal distribution in daily stress levels was observed, with peaks at stress



**Figure 3: Correlation Between Stress and Busyness Levels.** Employing Pearson’s correlation coefficient, we observe a moderate positive correlation with an R2 value of 0.625. This finding suggests that, despite the variation in the distribution of participant daily survey responses, an increase in daily busyness is concomitant with an elevation in reported stress levels.

<b>Top 5 Most Stressful Dates:</b>	
December 10, 2023	- Average Stress Level: 10.0
December 2, 2023	- Average Stress Level: 10.0
December 14, 2023	- Average Stress Level: 9.5
November 3, 2023	- Average Stress Level: 9.0
December 12, 2023	- Average Stress Level: 9.0
<b>Top 5 Least Stressful Dates:</b>	
December 28, 2023	- Average Stress Level: 1.0
December 22, 2023	- Average Stress Level: 1.0
December 27, 2023	- Average Stress Level: 1.0
November 19, 2023	- Average Stress Level: 1.0
December 23, 2023	- Average Stress Level: 1.33
<b>Top 5 Most Busy Dates:</b>	
December 12, 2023	- Average Busyness Level: 9.5
November 16, 2023	- Average Busyness Level: 9.25
December 6, 2023	- Average Busyness Level: 9.0
December 19, 2023	- Average Busyness Level: 9.0
November 17, 2023	- Average Busyness Level: 9.0
<b>Top 5 Least Busy Dates:</b>	
December 22, 2023	- Average Busyness Level: 1.0
December 27, 2023	- Average Busyness Level: 1.0
November 26, 2023	- Average Busyness Level: 2.4
December 21, 2023	- Average Busyness Level: 2.5
December 20, 2023	- Average Busyness Level: 3.0
<b>Sleep Disruption for these Dates</b>	
Most Stressful Dates:	88.89%
Least Stressful Dates:	28.57%
Most Busy Dates:	60%
Least Busy Dates:	25%

**Figure 4: Summary of Key Stress and Busyness Metrics on Specific Dates.** The data revealed high-stress and high-busyness dates, with peak average stress levels reaching 10.0 and busyness levels up to 9.5 during these times. In contrast, the lowest stress and busyness periods averaged around 1.0. Periods of heightened stress and busyness coincided with midterms and finals, underlining the substantial influence of these academic events on student well-being. Conversely, notably lower stress and busyness were observed after finals and during the Thanksgiving break, suggesting a significant decrease in stress after major academic deadlines. These findings underscore a clear correlation between academic schedules and fluctuations in student stress.

levels of 2 and 8, suggesting days of both low and high stress among students (Figure 2). The study found a moderate positive correlation ( $R^2 = 0.625$ ) between the busyness and stress reported by students, indicating that increases in academic deadlines are likely to enhance stress levels (Figure 3).

Further analysis identified specific dates where stress and busyness levels peaked. The top five most stressful and busiest dates had average stress levels of 10.0 and busyness levels of 9.5, aligning with key academic deadlines (Figure 4). Conversely, the least stressful and busy periods, like the Thanksgiving break and post-finals, showed significantly lower stress and busyness levels, highlighting the impact of academic responsibilities on student well-being.

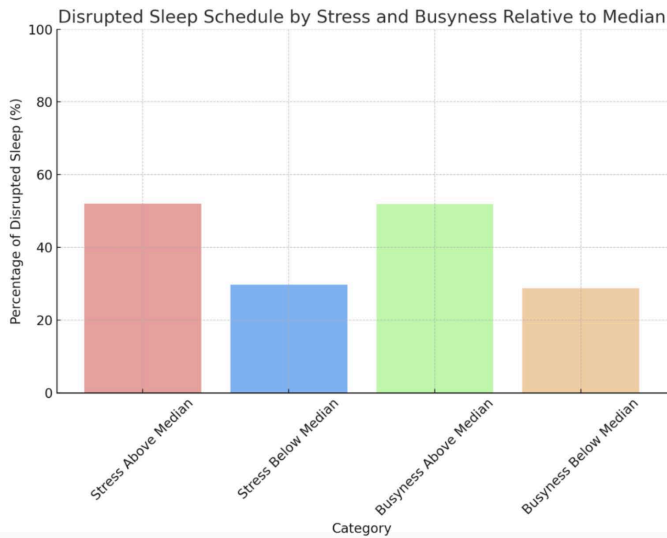


**Figure 5: Sleep Disruption Prevalence with Stress and Busyness Levels.** The analysis revealed a clear link between sleep disruption and higher stress and busyness levels. Specifically, 52% of participants experienced disrupted sleep when stress levels were above the median, compared to only 29.76% when below the median. Similarly, 51.90% reported sleep disruptions when busyness levels exceeded the median, versus 28.75% when below. These trends are further illustrated by the quartile distributions for stress and busyness: for stress, the 25th, 50th (median), and 75th quartiles were 3.0, 6.0, and 8.0, respectively; for busyness, these quartiles were 5.0, 6.0, and 8.0. These data indicate that days with higher stress and busyness are consistently associated with more sleep disturbances.

**Sleep Disruption Patterns:** The relationship between stress, busyness, and sleep disruptions was significant. On days when stress and busyness were above the median levels, over half of the participants (52%) reported disruptions in their sleep patterns, compared to less than a third (29.76%) on less stressful days (Figure 5). Higher quartile stress and busyness days saw a marked increase in sleep disturbances, with 79.31% of participants experiencing disrupted sleep when both factors exceeded the 75th percentile (Figure 6). Notably, the most stressful and busiest periods correlated with key academic timelines, particularly around midterms and finals.

The proportion of students reporting sleep disruptions was significantly higher during the top five most stressful days (88.89%) compared to the least stressful days (28.57%). A similar pattern was observed with busyness, where 60% reported disrupted sleep during the busiest days versus only 25% during less busy periods (Figure 7). These findings emphasize the direct impact of academic stress and busyness on student sleep quality, suggesting critical periods for targeted intervention to improve well-being.

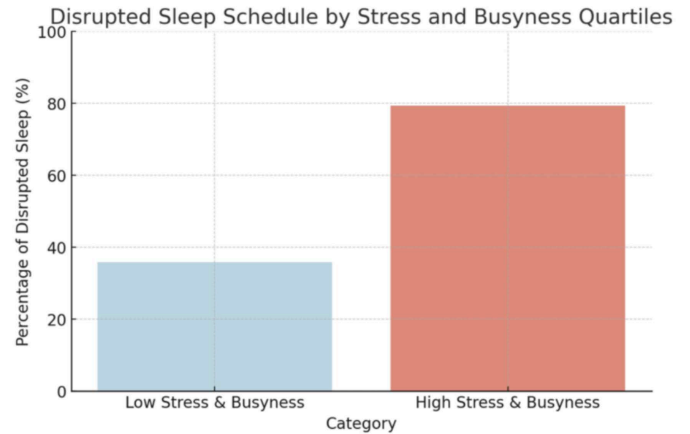


**Figure 6: Sleep Schedule Disruption Analysis by Stress and Busyness Quartiles.** An analysis of sleep disruptions in relation to the 25th (low) and 75th (high) stress and busyness quartiles indicated that sleep disruption is significantly more likely when both stress and busyness levels exceed the 75th quartile, with 79.31% reporting disturbances, compared to 35.90% when levels are at or below the 25th quartile.

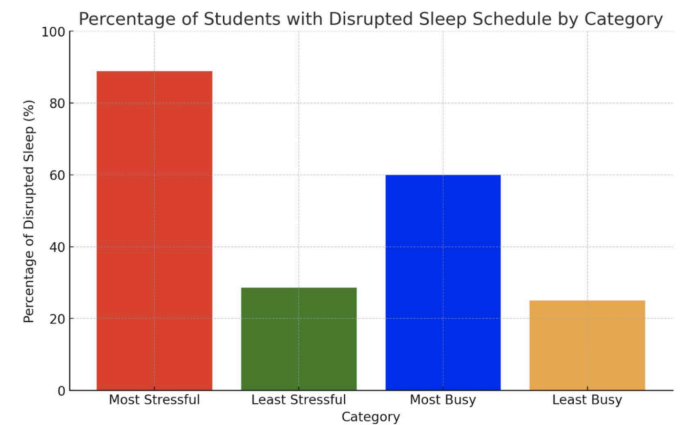


**Figure 7: Bar Graph of Sleep Disruption Percentages by Stress and Busyness Categories.** The analysis highlighted that the top five most stressful dates had stress levels peaking at 10.0, and the busiest days reached levels up to 9.5. In contrast, the least stressful and busy periods had levels as low as 1.0. Increased stress and busyness coincided with midterms and finals, significantly impacting student well-being. Conversely, stress and busyness dropped markedly after finals and during Thanksgiving break, correlating academic milestones with fluctuations in student stress levels.

**Conclusion**

The study highlights the effectiveness of digital phenotyping in a university setting to monitor and understand factors affecting student well-being. By integrating self-reported data with smartphone metrics, we can observe the real-time impacts of stress and busyness on sleep quality. These insights are crucial for developing personalized, data-driven interventions to mitigate mental health risks and enhance academic performance. Future research should focus on expanding digital phenotyping applications to predict and prevent student burnout, utilizing real-time data to tailor proactive and personalized interventions that improve productivity and overall quality of life.

**References**

Onnela, J. P., Rauch, S. (2016). Harnessing Smartphone-Based Digital Phenotyping to Enhance Behavioral and Mental Health. *Neuropsychopharmacol*, 41, 1691--1696. doi:10.1038/npp.2016.7.

Oudin, A., Maatoug, R., Bourla, A., Ferreri, F., Bonnot, O., Millet, B., Schoeller, F., Mouchabac, S., Adrien, V. (2023). Digital Phenotyping: Data-Driven Psychiatry to Redefine Mental Health. *J Med Internet Res*, 25, e44502. doi:10.2196/44502. PMID:37792430. PMCID:PMC10585447.

Melcher, J., Hays, R., Torous, J. (2020). Digital phenotyping for mental health of college students: a clinical review. *Evid Based Ment Health*, 23(4), 161--166. doi:10.1136/ebmental-2020-300180.

Egger, S. T., Knorr, M., Bobes, J., Bernstein, A., Seifritz, E., Vetter, S. (2020). Real-Time Assessment of Stress and Stress Response Using Digital Phenotyping: A Study Protocol. *Front. Digit. Health*, 2, 544418. doi:10.3389/fdgth.2020.544418.

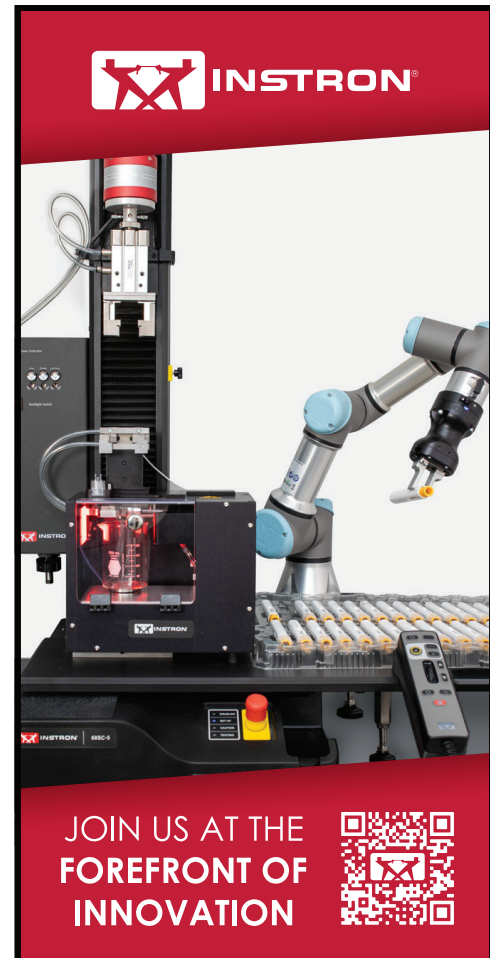
Roberts, M. E., Bell, E. A., Meyer, J. L. (2023). Mental health and academic experiences among U.S. college students during the COVID-19 pandemic. *Front Psychol*, 14, 1166960. doi:10.3389/fpsyg.2023.1166960. PMID:37187557. PMCID:PMC10176088.

Karyotaki, E., Cuijpers, P., Albor, Y., Alonso, J., Auerbach, R. P., Bantjes, J., Bruffaerts, R., Ebert, D. D., Hasking, P., Kiekens, G., Lee, S., McLafferty, M., Mak, A., Mortier, P., Sampson, N. A., Stein, D. J., Vilagut, G., Kessler, R. C. (2020). Sources of Stress and Their Associations With Mental Disorders Among College Students: Results of the World Health Organization World Mental Health Surveys International College Student Initiative. *Front. Psychol*, 11, 1759. doi:10.3389/fpsyg.2020.01759.

Ez ElArab, H., Rabie, M. A., Ali, D. H. (2014). Sleep behavior and sleep problems among a medical student sample in relation to academic performance: a cross-sectional questionnaire-based study. *Middle East Current Psychiatry*, 21(2), 72--80. doi:10.1097/01.XME.0000444452.76469.05.

Zeek, M. L., Savoie, M. J., Song, M., Kennemur, L. M., Qian, J., Jungnickel, P. W., Westrick, S. C. (2015). Sleep Duration and Academic Performance Among Student Pharmacists. *Am J Pharm Educ*, 79(5), 63. doi:10.5688/ajpe79563. PMID:26396272. PMCID:PMC4571043.

Do, S., Kwek, V., Saba, S., Dulchinos, A., Fletcher, R. (2023). MobilePath: A Mobile Server Platform for Health and Behavior Monitoring. *MIT Undergraduate Research Journal*, 45.



# Forming Hot Jupiters via Chaotic Tidal Migration

Donald Liveoak<sup>1</sup>, Prof. Sarah Millholland<sup>2</sup>

<sup>1</sup> Student Contributor, Class of 2025, Department of Physics, MIT, Cambridge, MA, 02139

<sup>2</sup> Supervisor, Department of Physics, MIT, Cambridge, MA, 02139

## Background

Extrasolar planets (“exoplanets”) are planets that orbit stars other than the Sun. Exoplanets exhibit an incredibly diverse range of properties and have transformed how we understand our Solar System and its context within the broader collection of planetary systems in the Galaxy. “Hot Jupiters” are massive, gaseous exoplanets that orbit very closely to their host stars, completing one orbit every few days. Their high masses and close proximity to their stars make them much easier to detect than other planets; in fact, they were the first type of exoplanets discovered (Mayor & Queloz, 1995).

Though many hot Jupiters have been observed, their ability to accrete mass and obtain extreme orbits remains poorly understood. Most exoplanet astronomers believe that hot Jupiters cannot form in their current orbits because the intense starlight creates a lack of solid materials to form the planet’s core (Dawson & Johnson, 2018). The leading theory is that these planets form in cold conditions far away from their host stars, where solid materials are abundant, and then migrate inwards.

A key piece of evidence for this mechanism is that many systems with hot Jupiters also host far-orbiting binary stars or large planets. These bodies can disrupt the initial “cold Jupiters” onto highly elliptical orbits. The elliptical (or “eccentric”) orbits force the planets to have very small pericenter distances (close approach distances) to their host stars. Strong tidal interactions distort the planet’s shape, leading to energy dissipation that causes the planet’s orbit to rapidly decay, circularize, and eventually reach the tight circular orbits we see today. This process is known as high eccentricity tidal migration.

Recently, a highly eccentric giant planet (TIC 241249530b) was discovered that is in the middle of high eccentricity tidal migration and will evolve over a few hundred million years to eventually become a hot Jupiter (Gupta, 2024). This planet is the second highly eccentric “warm Jupiter” discovered, providing evidence that some fraction of hot Jupiters are formed via high eccentricity migration. However, there is still much about this mechanism that remains a mystery, including details on how the migration occurs and the apparent deficiency of warm Jupiters in the high eccentricity phase, given that hot Jupiters are so common.

Importantly, previous work on TIC 241249530b does not consider tidally-induced vibrations within the interior of the planet, known as dynamical tides, which are excited when the orbits become highly eccentric. These vibrations have been shown to behave chaotically in certain circumstances, leading to episodes of strongly efficient energy dissipation (as the planet’s interior is stretched and squeezed) and rapid migration. This

process is known as chaotic tides, and because of its stochastic nature, it has been challenging to determine the implications of this process on observed warm Jupiters.

In this project, we investigate chaotic tides and their influence on TIC 241249530b’s dynamical history. We use a novel analytic approach to develop a model for determining the general outcome of chaotic migration. Based on this model, we present a chaotic migration formation history that replicates the parameters of TIC 241249530b.

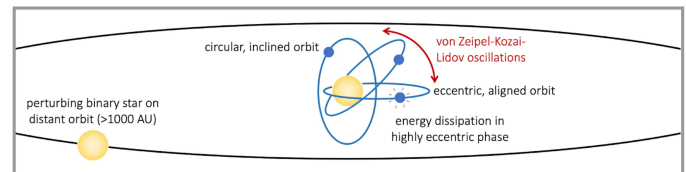


Fig. 1. Schematic diagram of vZLK oscillations.

## Analytics

The orbital eccentricity  $e$  describes the degree of elongation of the planet’s orbit and ranges from 0 to 1, with  $e = 0$  corresponding to a circular orbit and  $e \approx 1$  corresponding to a highly elliptical orbit. When considering systems with more than one orbiting body, the mutual inclination  $i$  is the angle between the two orbits.

One way for the giant planet to reach a highly eccentric orbit is through von Zeipel-Lidov-Kozai (vZLK) oscillations, which occur when the orbit of a large celestial body (the “perturber”) is highly inclined to the planet’s orbit (Naoz, 2016). vZLK oscillations result in periodic exchanges between the planet’s orbital eccentricity and mutual inclination (see Figure 1) in a way that approximately conserves the quantity

$$\sqrt{1 - e^2} \cos(i) \approx \text{constant}$$

The TIC 241249530 system hosts a perturbing binary star on a distant orbit, making it likely that TIC 241249530b’s high eccentricity results from vZLK oscillations. For a sufficiently large mutual inclination of  $\sim 90^\circ$ , vZLK oscillations would have driven the planet’s orbit to a high enough eccentricity to trigger chaotic tides (Vick, 2019).

Vick et al. (2019) derived a condition for chaotic migration to occur based on how close the planet comes to its star during its orbit. Specifically, chaotic migration begins when the pericenter distance  $r_p$  is smaller than some critical value that scales with planet properties as

$$r_{p,crit} \sim (1 - e)^{-0.135} \left( \frac{R_p}{R_j} \right) \left( \frac{10^3 M_p}{M_*} \right)^{-0.297}$$

where  $e$  is the eccentricity of the orbit when chaotic migration begins,  $R_p$  is the radius of the planet,  $R_j$  is the radius of Jupiter,  $M_p$  is the mass of the planet, and  $M_*$  is the mass of the star. Notably,  $r_{p,crit}$  is only strongly dependent on the planet's orbital eccentricity and intrinsic properties of the system, meaning that it can be determined without the need for simulations.

Our key insight is that the critical pericenter distance  $r_{p,crit}$  determines when chaotic migration ends. This is because angular momentum is conserved during chaotic migration, meaning that the pericenter distance is approximately constant. This observation provides a simple means of estimating the post-migration pericenter distance of planets undergoing chaotic migration. Since  $r_p$  is approximately constant in the subsequent tidal interactions due to the conservation of angular momentum, this allows us to estimate the pericenter distance at all later times.

To demonstrate that  $r_{p,crit}$  is a precise estimate for the post-migration pericenter distance, we performed a series of simulations. We modeled vZLK oscillations using the open-source software package KozaiPy, which is designed to perform gravitational dynamics simulations (Muñoz, 2016). KozaiPy assumes that the planetary and stellar masses are averaged across their orbits (the “secular approximation”) and that the inner orbit is much smaller than the outer orbit (the “hierarchical approximation”). We modified KozaiPy to include the effects of dynamical tides using the formulation from Vick et al. (2019).

Figure 2 shows the post-migration pericenter distance for a set of simulations that used different values for the planet's radius. The simulations performed using KozaiPy agree well with the analytic estimate, demonstrating that the estimate is a powerful means of calculating the planet's post-migration location.

After chaotic migration ends, the planet's angular momentum is conserved in subsequent tidal interactions, implying that the pericenter distance is also approximately conserved. This

conservation allows full prediction of the planet's migration over time. This information was used to piece together the history of TIC 241249530b. Evaluating  $r_{p,crit}$  with the present-day radius and mass of TIC 241249530b yields a post-migration pericenter distance of no more than  $r_p \approx 0.018$  astronomical units (AU). However, this is less than half of the planet's observed pericenter distance  $r_p \approx 0.038$  AU (red dot in Figure 2). Thus, assuming the planet's present-day radius, the planet was predicted to have migrated much closer to its star than it actually did.

Based on Figure 2 and our equation for  $r_{p,crit}$ , this inconsistency is resolved by assuming that TIC 241249530b's radius was inflated sometime during its history and contracted after migrating. In order to reconcile the observed eccentricity and pericenter distance of the planet, its radius must have been inflated to

$R_p \gtrsim 2.4R_j$ , which is twice its present-day value of  $R_p \approx 1.19R_j$ . With this assumption, we confirmed using KozaiPy simulations (Figure 3) that for  $R_p = 2.6R_j$ , chaotic migration led to a planet with an eccentricity of  $e \approx 0.94$  and pericenter distance  $r_p \approx 0.038$  AU, which matches the observed parameters of TIC 241249530b.

The mechanisms that caused the planet's radius to rapidly inflate and deflate remain unclear. The radius evolution is partially accounted for by a gas giant's standard cooling history; that is, planets form hot with large radii and then cool and contract to smaller radii (Hubbard, 1977). However, this effect only accounts for a relatively small inflation to at most  $R_p \approx 1.5R_j$  (Müller & Helled, 2021), which is insufficient to explain the large discrepancy between the observed radius ( $R_p \approx 1.19R_j$ ) and that required for chaotic migration to occur. Since deposition of energy into a planet's atmosphere is known to result in radius inflation, we hypothesize that the primary cause of the additional radius inflation is the energy deposited into the planet due to friction during extreme tidal interactions with its star (Thorngren, 2021). Using hydrodynamical models of the interior of gas giants, we plan to develop new models accounting for tidal heating-induced radius inflation and developing models considering this phenomenon will improve our predictions of tidal migrations for hot Jupiters.

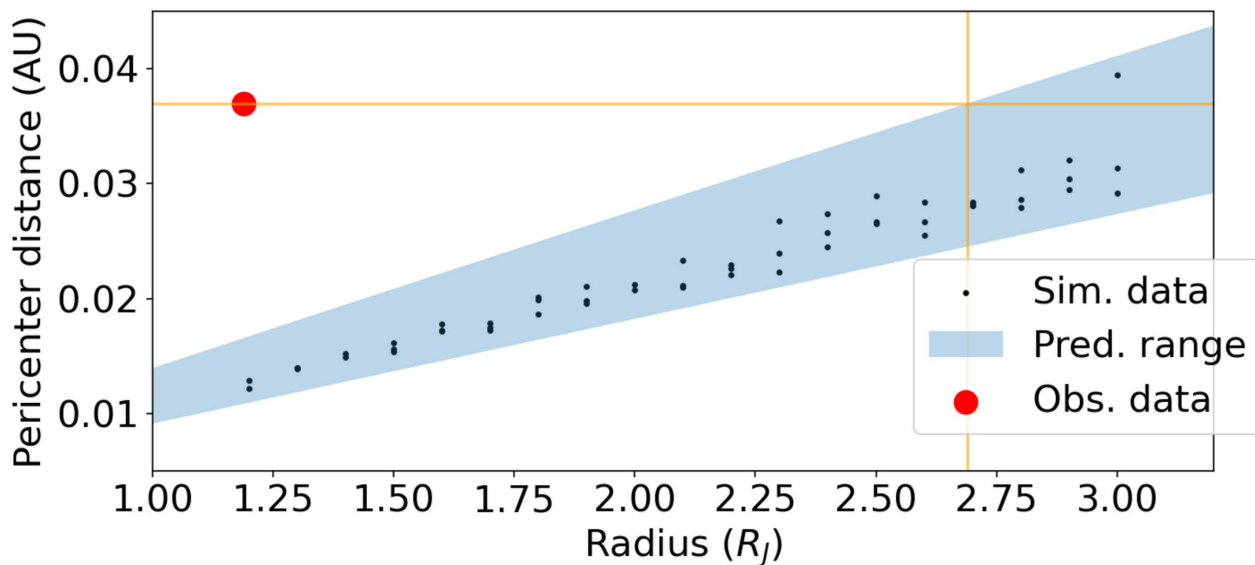


**Fig. 2. Pericenter distance at which chaotic migration ends vs. the planet's radius.** The black dots result from simulations of chaotic migration induced by vZLK oscillations. The light blue shaded region corresponds to the range of critical pericenter distances, with eccentricities ranging from 0.9 to 0.997. The physical parameters, such as the mass of the planet and perturbation, were chosen to be consistent with those measured by Gupta et al. (2024). The red circle indicates the pericenter distance and radius observed by Gupta et al. (2024) and falls outside of the parameter space compatible with chaotic migration. The orange lines indicate the pericenter distance of TIC 241249530b and the minimum radius required to attain this pericenter distance via chaotic migration.



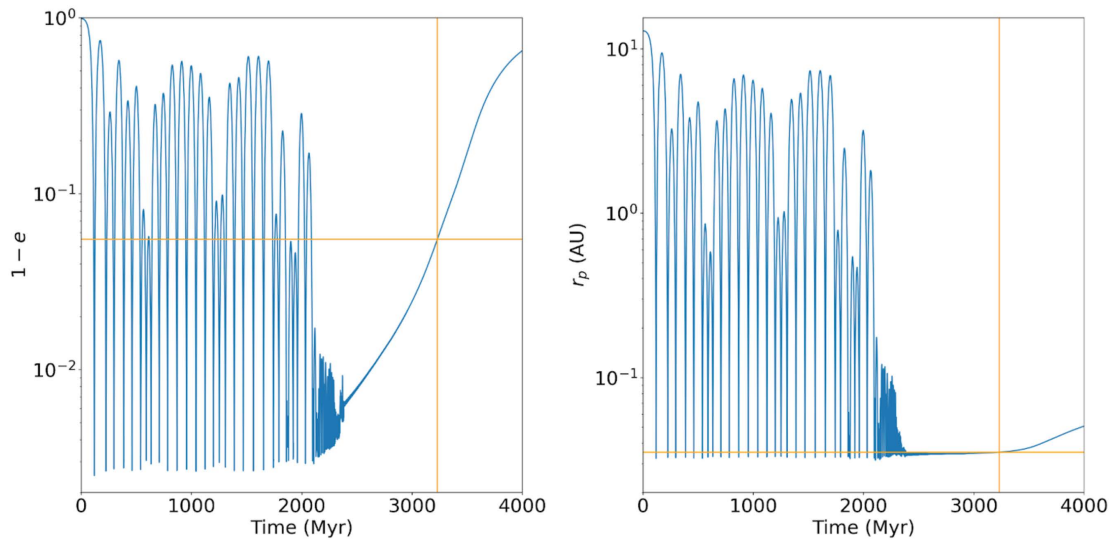


**Fig. 3. Blue: eccentricity and pericenter distance evolution from KozaiPy simulation for  $R_p=2.6R_J$ .** Orange: observed eccentricity, pericenter distance, and age of TIC 241249530b, as determined by Gupta et al. (2024). space compatible with chaotic migration. The orange lines indicate the pericenter distance of TIC 241249530b and the minimum radius required to attain this pericenter distance via chaotic migration.

We derived a novel analytic approach to understanding chaotic tidal migration in hot Jupiter systems and confirmed it with numerical simulations. Furthermore, by demonstrating that TIC 241249530b could not have migrated to its current orbit without undergoing significant radius inflation, we have not only clarified the formation history of this particular planet but also furthered formation models for hot Jupiters. This research demonstrates the importance of chaotic migration as a key pathway for hot Jupiter formation. Also, it provides a framework for future investigations into the dynamical histories of hot Jupiters, contributing to a deeper understanding of some of the earliest discovered exoplanets in the Galaxy.

## References

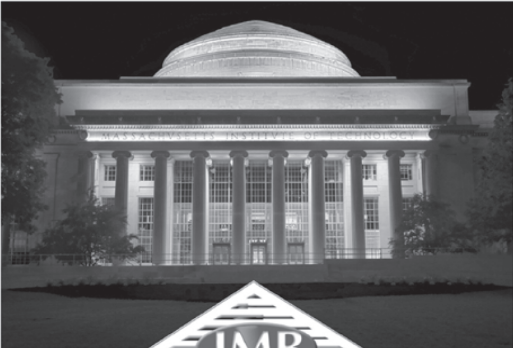
- Dawson, R. and Johnson, J. A. (2018). Annual Review of Astronomy and Astrophysics 56, 175-221. Retrieved on 10-15-2024 from [annualreviews.org](https://annualreviews.org)
- Gupta, A.F., Millholland, S.C., Im, H. et al. (2024). Nature 632, 50-54. Retrieved on 10-15-2024 from [nature.com](https://nature.com)
- Hubbard, W.B. (1977). Icarus 30, 305-310. Retrieved on 10-15-2024 from [sciencedirect.com](https://sciencedirect.com)
- Mayor, M. and Queloz, D. (1995.) Nature 378, 355-359. Retrieved on 10-15-2024 from [nature.com](https://nature.com)
- Müller, S., Helled, R. (2019). Monthly Notices of the Royal Astronomical Society 507, 2094-2102. Retrieved on 10-25-2024 from [academic.oup.com](https://academic.oup.com)
- Muñoz, D. (2016.) KozaiPy [Computer software]. Retrieved on 11-17-2024 from <https://github.com/djmunoz/kozaipy>
- Naoz, Smadar. (2016). Annual Review of Astronomy and Astrophysics 54, 441-489. Retrieved on 10-31-2024 from [annualreviews.org](https://annualreviews.org)


Thorngren, D. P., Fortney, J. J., Lopez, E. D., Berger, T. A., & Huber, D. (2021). Slow Cooling and Fast Re-inflation for Hot Jupiters. The Astrophysical Journal Letters, 909(1), L16.

Vick, M., Lai, D., Anderson, K.R. (2019). Monthly Notices of the Royal Astronomical Society 484, 5646-5668. Retrieved on 10-25-2024 from [academic.oup.com](https://academic.oup.com)

Electrical Construction ♦ Fire Alarm ♦ Special Projects ♦ Tel-Data/Security Systems

## Proud to Help Build A Bright Future for MIT





**J. & M. BROWN COMPANY, INC.**  
Excellence in electrical construction

**SPECTRUM**  
Integrated Technologies

Member of  
**NECA**  
GREATER BOSTON

Dedham, MA Tel:617.522.6800 [www.jmbco.com](http://www.jmbco.com)

# Barriers to Innovation: An Interview-Based Study of Opioid Startups and Industry Stakeholders

Riley Davis<sup>1</sup>, Vivian Lee<sup>2</sup>, David Santana<sup>1</sup>, Zen Chu<sup>3</sup>, Freddy Nguyen<sup>4</sup>

1 Student Co-First Author, Department of Electrical Engineering and Computer Science, MIT, Cambridge MA 02139

2 Student Co-First Author, Wellesley College, Wellesley MA 02481

3 Supervisor, Sloan School of Management, MIT, Cambridge MA 02142

4 Principal Investigator, Sloan School of Management, MIT, Cambridge MA 02142

The opioid epidemic has devastated communities across the U.S., with addiction and overdose rates skyrocketing due to both prescription opioid misuse and the prevalence of illicit opioids such as fentanyl. In response to this crisis, there has been a surge in innovations aimed at improving pain management alternatives, treatment methods for addiction, and harm reduction strategies. Startups addressing the opioid epidemic play a key role in these efforts by developing novel treatments, technologies, and approaches.

This study examines the complex dynamics of government regulation, public perception, and funding in the opioid industry, emphasizing the differing impacts on startups versus large corporations. Based on expert interviews, this research highlights regulatory, societal, and financial barriers that hinder opioid startups while favoring established corporations. Policy recommendations and strategies to enhance public awareness are discussed to promote equitable support for innovative solutions.

The study utilized a qualitative sampling approach, focusing on perspectives from policymakers, researchers, and entrepreneurs. Four structured interviews with six experts were conducted between March and June 2024, exploring regulatory, public perception, and funding issues in the opioid startup industry. David Rosenbloom, Professor of Public Health at Boston University, was selected for his role on the Opioid Recovery and Remediation Fund Advisory Council and his experience with opioid-focused startups. Abigail Kim, Policy Director at the Bureau of Substance Addiction Services (BSAS), provided insights into government responses and addiction policy. Dr. Alexander Walley and Dr. Simeon Kimmel, both affiliated with Boston Medical Center, contributed research-based perspectives on opioid addiction treatment. Margaux Babineau, Director of Marketing at MatTek Life Sciences, and Kevin O'Handley, CEO of Javelin Biotech, were chosen for their direct experience with healthcare startups, providing insight into the public and regulatory landscape startups must navigate. Interviews were guided by a structured outline (see supplementary table) and analyzed thematically, organizing insights into the core areas of regulation, perception, and funding.

Each interviewee brought unique perspectives illuminating the industry's challenges and opportunities. For instance, the consensus among experts indicated that government regulation significantly shapes the opioid industry. Companies must navigate legal frameworks while addressing critical health and societal issues, presenting considerable challenges for both large and small companies. Startups aiming to tackle the opioid epidemic encounter substantial barriers when seeking approval for

innovative solutions, particularly those focused on harm reduction measures such as overdose prevention centers. Legislation often hinders the adoption of new technologies and proven interventions, leading to limited public awareness and prevalent misconceptions about their benefits. This challenge is exemplified by the limited use and persistent admonishment of safe injection sites, a harm-reduction strategy that has been widely studied but still remains underutilized (Beletsky, 2008). Furthermore, the current regulatory landscape tends to favor large pharmaceutical corporations. Governments prefer to direct funding toward institutions they have previously worked with rather than new and innovative companies (Kim, personal communication, 2024). Interviewees emphasized that this dynamic stifles innovation and creates an uneven playing field for new entrants striving to offer alternative solutions to the opioid crisis, ultimately limiting potential contributions to the pharmaceutical industry and hampering the development of innovative patient care approaches.

Harm reduction strategies face additional obstacles from societal stigma, limiting public acceptance and the effective implementation of life-saving interventions. Interview insights indicate that having a person present during opioid use reduces mortality rates more effectively than naloxone access alone (Kim, personal communication, 2024). However, the stigma associated with drug use has impeded the establishment of safe injection sites, as governmental permission for the development of such facilities has historically been withheld. Similarly, the distribution of clean needles and other necessary supplies has been proven to save lives, yet many perceive these initiatives as facilitating and encouraging drug use (López-Ramírez, 2023). Societal attitudes that suggest individuals must "work for sobriety" undermine the idea that harm reduction services should be integral components of the healthcare system (Kim, Walley, & Kimmel, personal communication, 2024). This perspective not only hinders support for those in need but also complicates the efforts of startups introducing effective harm reduction interventions for the opioid crisis.

Lobbyists frequently engage with government entities to secure funding for various initiatives, influencing the competitive landscape for startups by directing resources and shaping policies that may prioritize larger corporations over innovative harm-reduction solutions. According to Kim, a common lobbying initiative aims to secure funding for the distribution of overdose reversal medication. Efforts include securing funding for the distribution of current medication as well as shifting to the

Challenge area	Topics discussed	Sample questions
<b>Regulatory Challenges</b>	<ol style="list-style-type: none"> <li>1. Evolving Regulations</li> <li>2. Compliance</li> </ol>	<ul style="list-style-type: none"> <li>• How have recent government regulations affected opioid treatment startups?</li> <li>• What licensing barriers impact addiction treatment facilities and telehealth services?</li> <li>• How can policymakers support harm reduction efforts?</li> </ul>
<b>Public Perception Challenges</b>	<ol style="list-style-type: none"> <li>1. Stigma and Misconceptions</li> <li>2. Education Needs</li> </ol>	<ul style="list-style-type: none"> <li>• How does public perception affect adoption of harm reduction and treatment programs?</li> <li>• What common misconceptions surround addiction treatment medications?</li> <li>• What strategies can help increase public understanding and acceptance of innovative addiction treatment methods?</li> </ul>
<b>Funding Challenges</b>	<ol style="list-style-type: none"> <li>1. Investment and Sustainability</li> <li>2. Commercialization Concerns</li> </ol>	<ul style="list-style-type: none"> <li>• What are the funding challenges specific to addiction treatment startups compared to general healthcare startups?</li> <li>• How do different funding structures affect the landscape?</li> </ul>

**Table 1. Core challenges and discussion topics identified in structured interviews with policymakers, researchers, and entrepreneurs in the opioid startup industry:** The table highlights key regulatory, public perception, and funding issues, along with sample questions guiding the exploration of these challenges.

distribution of 8 mg (in lieu of 4 mg) Naloxone nasal spray. This change in dosage does not change the efficacy of the treatment and is likely lobbied purely to increase drug sales (Kim, personal communication, 2024). According to the CDC, the 8 mg dose has shown a higher prevalence of opioid withdrawal signs and symptoms compared to the 4 mg dose (Payne, 2024). This emphasis on high-profit solutions often overshadows more impactful, less profitable options, thereby complicating funding access for startups focused on genuine, cost-effective solutions to the opioid crisis (Kim, personal communication, 2024).

Through structured interviews and thematic analysis, this study highlights the significant obstacles facing startups working to address the opioid epidemic, including stringent regulations, negative public perception, and complex funding dynamics. While larger corporations may benefit from regulatory advantages and established public trust, startups and early-stage research at medical centers and universities encounter significant barriers that impede innovation and development.

Given the escalating death toll associated with the opioid epidemic, swift and decisive action is imperative. By reducing unnecessary hurdles, governments can allow startups to implement strategies that have shown promise in preliminary trials and real-world settings to save lives. Fostering a supportive ecosystem for startups tackling the opioid crisis is essential. The convergence of regulatory reform, improved public perception, and enhanced funding mechanisms can empower startups to deliver innovative and life-saving solutions addressing the urgent needs of those affected by the opioid crisis. Coordinated efforts across government, industry, academia, health systems, and society are crucial to reversing this public health emergency.

### References

Beletsky, L., Davis, C. S., Anderson, E., & Burris, S. (2008). The Law (and Politics) of Safe Injection Facilities in the United States. *American Journal of Public Health, 98*(2), 231–237. <https://doi.org/10.2105/ajph.2006.103747>

López-Ramírez, E., Huber, M. J., Matías-Pérez, D., Santos-López, G., & Iván Antonio García-Montalvo. (2023). Opioid harm reduction and stigma: proposed methods to improve the perception of people with addiction. *Frontiers in Psychiatry, 14*. <https://doi.org/10.3389/fpsy.2023.1197305>

Payne, E. R., Stancliff, S., Rowe, K., Christie, J. A., & Dailey, M. W. (2024). Comparison of Administration of 8-Milligram and 4-Milligram Intranasal Naloxone by Law Enforcement During Response to Suspected Opioid Overdose — New York, March 2022–August 2023. *MMWR Morbidity and Mortality Weekly Report, 73*(5), 110–113. <https://doi.org/10.15585/mmwr.mm7305a4>

# Trust-building Hierarchical Automation Validating the Transfer of Perovskite Properties Across Scales

Kanokwan Tungkitkanchaen<sup>1</sup>, Alexander Siemenn<sup>2</sup>, Professor Tonio Buonassisi<sup>3</sup>

<sup>1</sup> Student Contributor, Class of 2025, Department of Mechanical Engineering, MIT

<sup>2</sup> Direct Supervisor, Department of Mechanical Engineering, MIT

<sup>3</sup> Principal Investigator, Department of Mechanical Engineering, MIT

In the age of climate change, the need for sustainable energy solutions is more urgent than ever, driving the demand for accelerated development of new materials (Intergovernmental Panel on Climate Change, 2023). Among potential materials, perovskite semiconductors stand out due to their high efficiency and cost-effectiveness in photovoltaic (solar cell) applications, which convert sunlight into electricity (Figure 1). However, increasing automation in research workflows can sometimes deviate from trusted, conventional techniques, potentially leading to skepticism among experts (Szymanski, 2023; Leeman, 2024). This project aims to build trust in ultra-high-throughput, autonomous materials synthesis methods that can significantly advance the discovery of energy materials to mitigate climate change.

We aim to test and validate a novel tool, DiSCO (Discovery, Synthesis, Characterization, and Optimization), specifically designed for synthesizing and characterizing perovskite semiconductors. DiSCO currently operates at a low-fidelity level, allowing for rapid, high-throughput synthesis and characterization. However, our goal is to validate its fidelity to elevate DiSCO to high fidelity, enabling it to maintain throughput while delivering high-quality, accurate results. Taken together, Figures 2 and 3 illustrate the DiSCO workflow developed in our lab, highlighting how material quality and automation levels influence throughput, which is why we are testing for specific characteristics.

By showing that perovskite materials synthesized with high-automation tools like DiSCO can retain key properties when scaled to higher-fidelity synthesis methods (such as non-automated spin-coating), we aim to demonstrate DiSCO's potential as a rapid yet reliable option, accelerating sustainable materials research. This project will employ high-throughput combinatorial synthesis methods to create new perovskite compounds and evaluate their properties across various synthesis scales, from initial low-fidelity samples to high-fidelity thin films, to determine scalability and effectiveness.

This project is divided into four key stages: synthesis, characterization, validation, and analysis (Figure 4). Each stage is critical to ensuring that materials synthesized by the DiSCO system meet the high standards of manually synthesized materials.

The synthesis process begins with preparing perovskite precursor solutions—liquid mixtures containing the chemical components needed to form perovskites. These solutions are loaded into DiSCO for 8-dimensional combinatorial synthesis, enabling the creation of a broad range of perovskite compositions. By precisely adjusting the ratios of formamidinium (FA), methylammonium (MA), lead, iodine, cesium, bismuth, antimony, and bromine, we can systematically explore novel compositions at unprecedented scale and speed.

Following synthesis, high-fidelity characterization of the perovskite materials is essential to assess their structural and functional properties. This process will include characterizing DiSCO-synthesized perovskites as droplets (via inkjet printing) using techniques such as X-ray diffraction (XRD), scanning electron

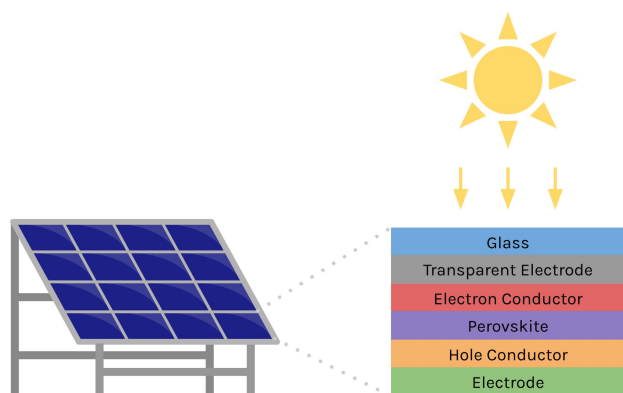


**Fig. 1. Perovskite solar cell structure: sunlight passes through glass and a transparent electrode to reach the perovskite layer, generating charge carriers. These carriers are directed by electron and hole conductors to the electrodes, producing electricity.**

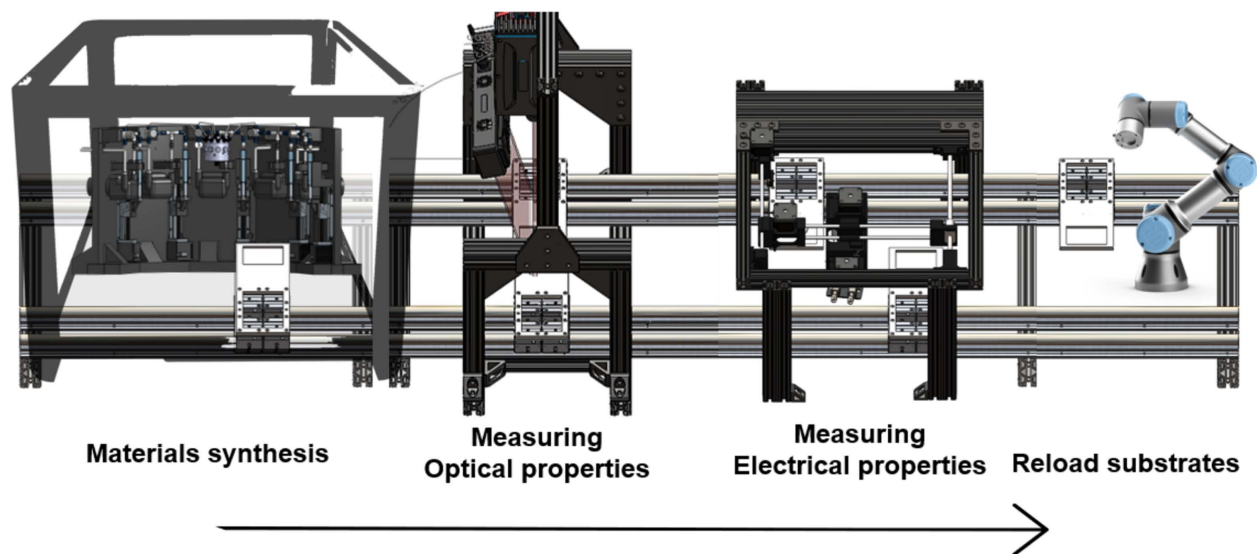


Fig. 2. DiSCO workflow: an automated sequence for high-throughput perovskite synthesis and characterization, including materials synthesis, optical and electrical property measurement, and substrate reloading.

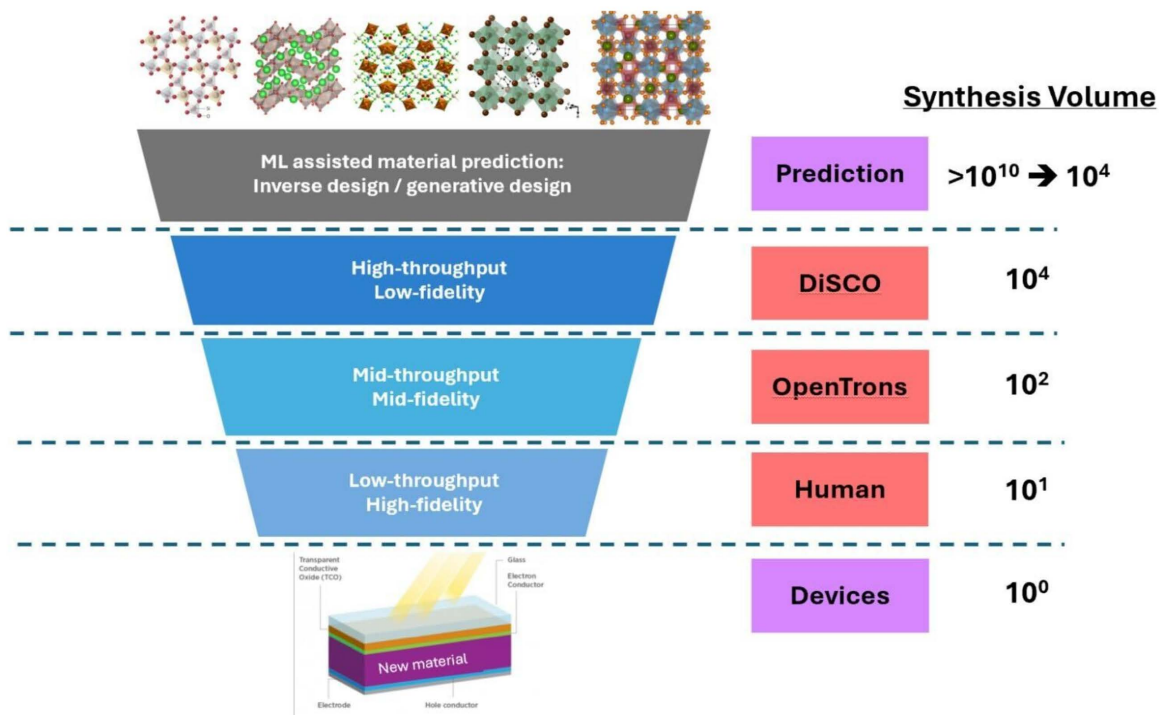
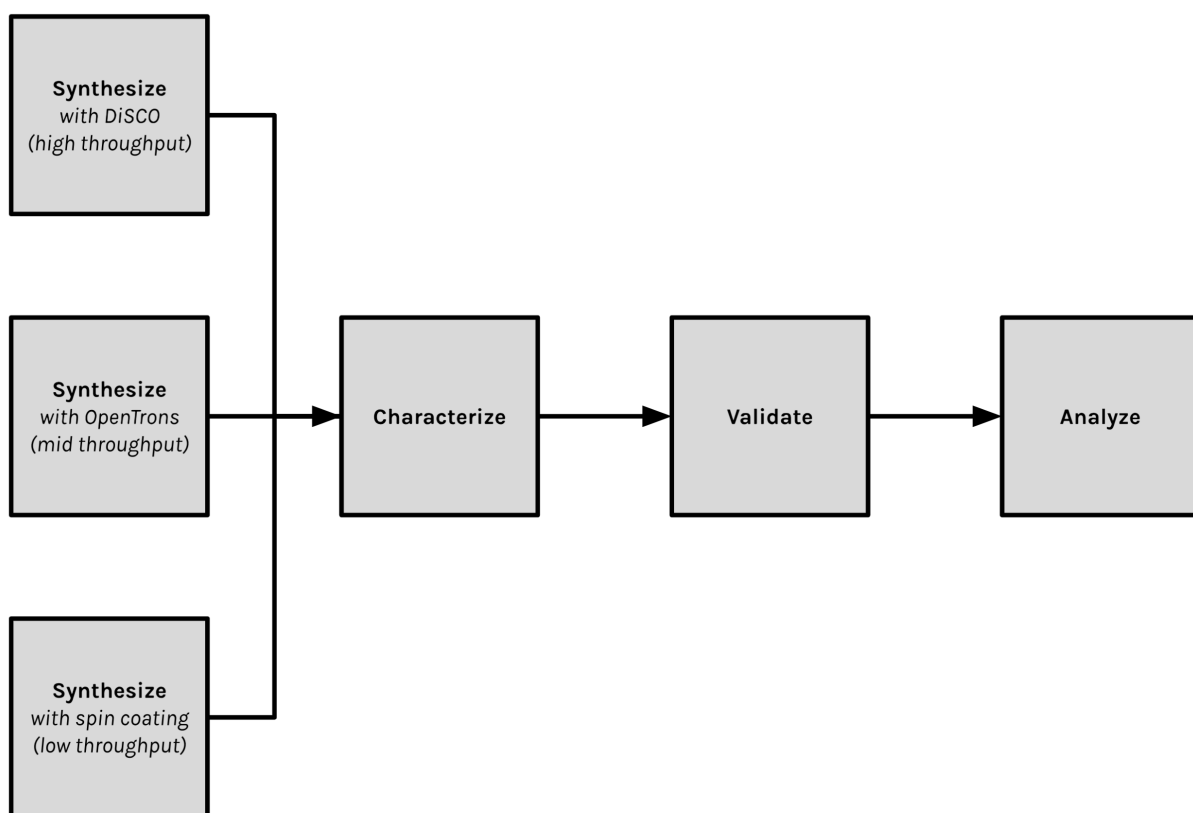


Fig. 3. Hierarchical Automation Levels: Comparison of synthesis methods from high-throughput, low-fidelity automation (DiSCO) to low-throughput, high-fidelity human techniques.



**Figure 4. Workflow for Material Synthesis and Characterization:** The process begins with synthesis, followed by dual characterization using DiSCO and OpenTrons. The results are then validated and analyzed, providing insights into the material's properties and potential for application.

microscopy (SEM), and energy-dispersive X-ray spectroscopy (EDS). Equivalent high-fidelity characterization will be performed on thin films synthesized using conventional methods like OpenTrons and spin coating, allowing us to compare high-throughput and traditional methods.

Validating the DiSCO system is crucial for building trust in the synthesized materials. Validation involves creating a known perovskite material within an 8-dimensional composition space, manipulating the concentrations of eight essential elements—both cations and anions—forming the perovskite structure. This space includes mixed cations such as FA, MA, cesium, bismuth, and antimony, and mixed anions like iodine and bromine, alongside lead. While each component has been studied in simpler combinations, this is among the first attempts to optimize all eight together as a full octonary (eight-component) system. Unexpected results will be monitored and addressed to improve reproducibility. Successful validation will confirm DiSCO's readiness for reliable material discovery.

The analysis will compare results from high-throughput synthesis (DiSCO) with those from semi-automated (OpenTrons) and traditional methods. Key properties such as crystallographic phase (XRD), morphology (SEM), chemical composition (EDS), band gap, photoluminescence, and conductivity will be examined to assess how closely DiSCO-synthesized materials match conventionally synthesized ones. This analysis will provide essential insights into scalability and inform future improvements.

So far, we have observed strong transferability for specific critical properties. Organic perovskites synthesized using DiSCO

demonstrate over 95% cosine similarity in optical reflectance, showing that the automated synthesis closely replicates the light-absorbing characteristics of manually synthesized counterparts, which is essential for photovoltaic efficiency. Additionally, we observed a band gap differential of less than 0.03 eV between DiSCO-synthesized and manually synthesized samples. Since the band gap is fundamental to a material's ability to absorb light and generate electricity, this minimal difference confirms that DiSCO can accurately replicate the electronic properties crucial for energy conversion efficiency.

However, replicating certain structural properties, particularly morphology, across different automation scales remains challenging. Crystallographic phase transferability also varies based on the composition being studied. Moving forward, we will refine synthesis and characterization processes to improve reproducibility for challenging properties like morphology. By further validating DiSCO and enhancing transferability across all material properties, we aim to accelerate the discovery and development of high-performance perovskite materials for renewable energy applications.

## References

Leeman, John, Liu, Yan, Stiles, Jack, Lee, Sarah, Bhatt, Priya, Schoop, Lisa, et al. (2024). Challenges in high-throughput inorganic material prediction and autonomous synthesis. ChemRxiv. Retrieved on November 8, 2024, from <https://doi.org/10.26434/chemrxiv-2024-5p9j4>

Szymanski, Nicholas J., Rendy, Brian, Fei, Ying, et al. (2023). An autonomous laboratory for the accelerated synthesis of novel materials. *Nature*, 624, 86–91. Retrieved on November 8, 2024, from <https://doi.org/10.1038/s41586-023-06734-w>

Ahmed, Md Tawhid, Islam, Saif, & Ahmed, Farzana. (2023). Exchange-correlation functional's impact on structural, electronic, and optical properties of (N2H5)PbI3 perovskite. *Heliyon*, 9(7), e17779. Retrieved on November 8, 2024, from <https://www.science-direct.com/science/article/pii/S2405844023049873>

Intergovernmental Panel on Climate Change. (2023). AR6 Synthesis Report: Summary for Policymakers. Retrieved on November 8, 2024, from <https://www.ipcc.ch/report/sixth-assessment-report-cycle>

#GSKBoston

Uniting talent  
and technology  
to drive innovation.



GSK

[gskboston.com](https://gskboston.com)

# MURJ Reports



# Depth-first Search for Tensor Rank and Border Rank Over Finite Fields

Jason Yang<sup>1</sup>, Virginia Vassilevska Williams<sup>2</sup>

<sup>1</sup> Student Contributor, MIT Class of 2025, Department of Electrical Engineering and Computer Science, Cambridge, MA 02139

<sup>2</sup> Supervisor, Department of Electrical Engineering and Computer Science, Cambridge, MA 02139

**WE PRESENT AN  $O^*(|\mathbb{F}|^{(R-n_*)\sum_d n_d + n_*})$ -TIME ALGORITHM FOR DETERMINING WHETHER A TENSOR OF SHAPE  $n_0 \times \dots \times n_{D-1}$  OVER A FINITE FIELD  $\mathbb{F}$  HAS RANK  $\leq R$ , WHERE  $n_* := \max_d n_d$ ; WE ASSUME WITHOUT LOSS OF GENERALITY THAT  $\forall d : n_d \leq R$ . WE ALSO EXTEND THIS PROBLEM TO ITS BORDER RANK ANALOG, I.E., DETERMINING TENSOR RANK OVER RINGS OF THE FORM  $\mathbb{F}[X]/(X^H)$ , AND GIVE AN  $O^*(|\mathbb{F}|^{H \sum_{1 \leq r \leq R} \sum_d \min(r, n_d)})$ -TIME ALGORITHM. BOTH OF OUR ALGORITHMS USE POLYNOMIAL SPACE.**

## 1. Introduction

Over an arbitrary ring  $R$  (i.e., a set with addition, multiplication, additive identity, and multiplicative identity, but not necessarily division), a *rank- $R$  canonical polyadic decomposition (CPD)* of a tensor (i.e., multidimensional array)  $T \in \mathcal{R}^{n_0 \times \dots \times n_{D-1}}$ , is a list of factor matrices  $A_d \in \mathcal{R}^{n_d \times R}$ ,  $0 \leq d \leq D$ , such that

$$\forall i_0, \dots, i_{D-1} : T_{i_0, \dots, i_{D-1}} = \sum_{0 \leq r < R} \prod_{0 \leq d < D} (A_d)_{i_d, r}.$$

This relation is commonly notated as  $T = \llbracket A_0, \dots, A_{D-1} \rrbracket$  or  $T = \sum_{0 \leq r < R} \otimes_d (A_d)_{:,r}$ . The rank of the tensor  $T$  is the smallest  $R$  such that there exists a rank- $R$  CPD of  $T$ .

Tensor rank is the central problem underlying fast matrix multiplication (MM), the main performance bottleneck of most linear algebra operations, backpropagation, various graph algorithms, and many other problems. Formally, the action of multiplying a  $m \times k$  matrix with a  $k \times n$  matrix can be described with a  $mk \times kn \times nm$ -shaped tensor  $\mathcal{M}_{(m,k,n)}$  then a rank- $R$  CPD of this tensor yields an  $O(N^{3 \log_{mk} R})$ -time algorithm for multiplying two  $N \times N$  matrices, for arbitrarily large  $N$  (Bläser, 2013). Thus, finding CPDs of  $\mathcal{M}_{(m,k,n)}$  tensors with smaller rank than previously known would lead to faster algorithms for MM, which makes tensor rank an important problem.

Usually  $R$  is the real numbers ( $\mathbb{R}$ ) or complex numbers ( $\mathbb{C}$ ), but setting it to a finite field can also be useful. For example, one can find a CPD of a tensor over a small finite field (often the integers mod 2), then lift to a larger ring such as  $\mathbb{Z}$ ; this is a common technique in fast MM (Fawzi et al., 2022; Kauers & Moosbauer, 2022), since CPDs over the integers are the most desired, for reasons such as reducing floating-point errors. Additionally, restricting  $R$  to a finite field gives some hope that obtaining an CPD is even possible, which other rings do not share: for example, a CPD using real numbers usually cannot be represented exactly; and finding tensor rank over the integers is known to be undecidable (Shitov, 2016). For these reasons, we are interested in working over finite fields.

We also want to broaden our scope to analyzing arbitrary tensors, not just MM tensors, as we want to know if general

algorithmic speedups exist. Additionally, tensor rank has applications outside of fast MM, such as the light bulb problem (Alman & Zhang, 2023) and dynamic programming (Alman et al., 2024).

Thus, our goal is to solve the following problem: given a finite field  $F$ , an arbitrary tensor  $T \in \mathbb{F}^{n_0 \times \dots \times n_{D-1}}$  and rank threshold  $R$ , return a CPD of  $T$  of rank  $\leq R$  if one exists, or prove that no such CPD exists. Although this problem is NP-complete (H<sup>\*</sup>astad, 1990), it may still be possible and useful to attain exponential speedup over brute force.

We require our algorithm to have guaranteed correctness, which most previous work does not satisfy: for example, (Courtois et al., 2011; Heule et al., 2019; Kauers & Moosbauer, 2022) use random search, and (Fawzi et al., 2022) uses reinforcement learning, none of which can prove that a CPD of specific rank does not exist.

To this end, we present an  $O^*(|\mathbb{F}|^{(R-n_*)\sum_d n_d + n_*})$ -time polynomial-space algorithm for this problem, where  $O^*$  suppresses polynomial factors and  $n_* := \max_d n_d$ ; here we assume WLOG that  $\forall i : n_i \leq R$ . For fixed  $R$  the time complexity is bounded above by  $O^*(|\mathbb{F}|^{D \cdot \frac{(R+n_*)^2}{4}})$ .

We also investigate *border* CPDs of exponent  $H$ , which are CPDs of a tensor  $x^{H-1}T$  over the ring  $\mathbb{F}[x]/(x^H)$ , where all elements in  $T$  are in  $\mathbb{F}$ ; such CPDs are also widely used in fast MM (more detail in Section 4). For this problem, we present an  $O^*(|\mathbb{F}|^{H \sum_{1 \leq r \leq R} \sum_d \min(r, n_d)})$ -time polynomial-space algorithm; for fixed  $R$  the time complexity is bounded above by  $O^*(|\mathbb{F}|^{HD \cdot \frac{R}{4}})$ .

The code for our algorithms is available at <https://github.com/coolcomputery/tensor-cpd-search>.

### 1.1 Notation

- Tensor slices are denoted with NumPy notation.
  - for a two-dimensional tensor  $A$ :  $A_{r,:}$  is the  $r$ -th row of  $A$ ;  $A_{:,c}$  denotes the submatrix containing the first  $c$  columns of  $A$ .

- The flattening of a tensor  $T$  is denoted as  $\text{vec}(T)$ , where elements are ordered in some consistent manner (e.g., row-major).
- The axis- $d$  (“mode- $d$ ”) unfolding of a tensor  $T$  is

$$T_{(d)} := \begin{bmatrix} \vdots \\ \text{vec}(T_{i_1, \dots, i_d, \dots, i_D}) \\ \vdots \end{bmatrix}_{i_d}$$

- The tensor product of tensors  $A$  and  $B$  is  $A \otimes B := [A_{i_0, \dots, i_{D-1}} B_{j_0, \dots, j_{D'-1}}]_{i_0, \dots, i_{D-1}, j_0, \dots, j_{D'-1}}$ .
- The axis- $d$  operation of  $T \in \mathcal{R}^{n_0 \times \dots \times n_{D-1}}$  by a matrix  $M \in \mathcal{R}^{n'_d \times n_d}$  is  $M \times_d T := [\sum_{i_d} M_{i'_d, i_d} T_{i_0, \dots, i_{D-1}}]_{i_0, \dots, i_{d-1}, i'_d, i_{d+1}, \dots, i_{D-1}}$ .
- A CPD with rank  $R$  (“rank- $R$  CPD”) is a list of factor matrices  $A_d \in \mathcal{R}^{n_d \times R}$ ,  $0 \leq d < D$  that evaluates to the tensor  $[[A_0, \dots, A_{D-1}]] := [\sum_{0 \leq r < R} \prod_d (A_d)_{i_d, r}]_{i_0, \dots, i_{D-1}} = \sum_r \otimes_d (A_d)_{:, r}$ .
- The rank of a tensor  $T$  is the smallest  $R$  such that  $T$  has a rank- $R$  CPD  $[[A_0, \dots, A_{D-1}]]$ , and is denoted as  $\text{rk}(T)$ . When  $T$  is a matrix, this definition coincides with matrix rank.
- The phrase “rank- $\leq R$  CPD” is short for “a CPD of rank at most  $R$ .”
- The reduced row echelon form of a matrix  $M$  is denoted as  $\text{rref}(M)$ .
- $\text{GL}(n, \mathbb{F})$  denotes the set of invertible  $n \times n$  matrices with elements in a field  $\mathbb{F}$ .

## 2. Axis-Reduction

Naïvely, finding a rank- $\leq R$  CPD of a tensor  $T \in \mathbb{F}^{n_0 \times \dots \times n_{D-1}}$  using brute force would take  $O^*(|\mathbb{F}|^{R \sum_d n_d})$  time, as such a CPD  $[[A_0, \dots, A_{D-1}]]$  contains  $Rn_0 + \dots + Rn_d$  many variables, each with  $|\mathbb{F}|$  many possible values.

By itself, this running time is not very good because each  $n_i$  could be arbitrarily large, even if  $R$  is small.

Here, we show that one can always transform  $T$  so that  $\forall d: n_d \leq R$  without affecting the existence of a solution.

For each axis  $d$ , define the following:

- the axis- $d$  unfolding of  $T$ , denoted as  $T_{(d)}$ , a matrix whose  $i$ -th row is the flattening of the slice  $T_{\underbrace{i_1, \dots, i_d, \dots, i_D}_d}$ , where all slices are flattened in the same manner
- an arbitrary change-of-basis matrix  $Q_d \in \text{GL}(n_d, \mathbb{F})$  such that  $Q_d T_{(d)} = \text{rref}(T_{(d)})$
- the axis- $d$  rank of  $T$ ,  $r_d := \text{rk}(T_{(d)})$

Then we create the new tensor  $T' = (Q_{D-1})_{:r_{D-1}} \times_{D-1} (\dots ((Q_0)_{:r_0} \times_0 T))$  which has shape  $r_0 \times \dots \times r_{D-1}$ . We call this process *axis-reduction*; note that each  $Q_d$  can be found using Gaussian elimination, so *axis-reduction* runs in polynomial time.

We have  $\text{rk}(T) = \text{rk}(T')$ , since  $T = (Q_0^{-1})_{:r_0} \times_0 (\dots ((Q_{D-1}^{-1})_{:r_{D-1}} \times_{D-1} T'))$  and doing axis

operations  $\times_d$  does not increase CPD rank. In fact, any CPD of  $T = [[A_0, \dots, A_{D-1}]]$ , can be transformed into an equal-rank CPD of  $T' = [[(Q_0)_{:r_0}, A_0, \dots, (Q_{D-1})_{:r_{D-1}}, A_{D-1}]]$ , and vice versa; so we can search for a CPD over  $T'$  and then transform it back to a CPD for  $T$ .

The upshot is that if  $T$  has a rank- $\leq R$  CPD  $[[A_0, \dots, A_{D-1}]]$ , it must satisfy  $\forall d: r_d \leq R$ : this is because each axis- $d$  slice  $T_{i_1, \dots, i_d, \dots, i_D}$  would equal  $\sum_r (A_d)_{i_d, r} (\otimes_{d' \neq d} (A_{d'})_{:, r})$ , so  $\text{span} \{T_{i_1, \dots, i_d, \dots, i_D}\}_{0 \leq i < n_d} \subseteq \text{span} \{(\otimes_{d' \neq d} (A_{d'})_{:, r})\}_{0 \leq r < R}$ . Therefore, if any  $r_d$  exceeds  $R$ , we immediately know that a rank- $R$  CPD of  $T$  does not exist.

Already, axis-reduction ensures that brute force runs within  $O^*(|\mathbb{F}|^{DR^2})$  time, because after replacing  $T$  with its axis-reduced version, every  $n_d$  is at most  $R$ . A more clever observation is that if we fix all first columns  $(A_d)_{:, 0}$  of the factor matrices, then  $T - \otimes_d (A_d)_{:, 0}$  must have rank  $\leq R - 1$ , so we can apply axisreduction again and recurse in a depth-first search fashion. Because  $\forall d: n_d \leq R$  after axis-reduction, the root call, which has rank threshold  $R$ , has at most  $|\mathbb{F}|^{DR}$  many children calls, each of which has rank threshold  $R - 1$ . Continuing this observation all the way down to calls with rank threshold 0, we end up making  $O(|\mathbb{F}|^{DR} \dots |\mathbb{F}|^{D-1}) = O(|\mathbb{F}|^{D(R+1)}) = O(|\mathbb{F}|^{D \frac{R+1}{2}})$  total calls. Since each call takes polynomial work, this depth-first-search algorithm runs within  $O^*(|\mathbb{F}|^{D(R+1)}) = O^*(|\mathbb{F}|^{D \frac{R+1}{2}})$  time, significantly faster than brute force. We use essentially the same algorithm to search for border CPDs in Section 4.

Finally, we note that axis-reduction can efficiently find rank- $\leq 1$  CPDs, using the fact that  $1^D = 1$ :

**Lemma 1.** *For any tensor  $T \in \mathbb{F}^{n_0 \times \dots \times n_{D-1}}$ ,  $\text{rk}(T) \leq 1$  if and only if  $\forall d: \text{rk}(T_{(d)}) \leq 1$ . Furthermore, if this condition is satisfied, a minimum-rank CPD of  $T$  can be found in polynomial time.*

## 3. Tensor Rank

Surprisingly, for regular CPD, it is possible to achieve our desired running time without explicitly using recursion, while only using axis-reduction once.

### 3.1 Algorithm

Assume that  $T \in \mathbb{F}^{n_0 \times \dots \times n_{D-1}}$  is axis-reduced and suppose a rank- $R$  CPD  $T = [[A_0, \dots, A_{D-1}]]$  exists; note that this implies  $\forall d: n_d \leq R$ .

Construct some  $Q \in \text{GL}(n_0, \mathbb{F})$  such that  $QA_0 = \text{rref}(A_0)$ .

Because

$$T_{(0)} = A_0 \begin{bmatrix} \vdots \\ \text{vec}(\otimes_{d \neq 0} (A_d)_{:, r}) \\ \vdots \end{bmatrix}_r,$$

$\text{rk}(A_0) = n_0$ , so we can assume  $\text{rref}(A_0) = [I_{n_0} | X]$  for some arbitrary matrix  $X$ , after simultaneously permuting the columns of all factor matrices appropriately.

Denote  $\tilde{T} := T - [[(A_0)_{:, n_0}, \dots, (A_{D-1})_{:, n_0}]]$ ; then  $Q \times_0 \tilde{T} = [[I_{n_0}, (A_0)_{:, n_0}, \dots, (A_{D-1})_{:, n_0}]]$ . For brevity, denote the right-hand side as  $\Xi$

Suppose  $\tilde{T}$  is fixed: to solve for  $Q$ , note that every axis-0 slice of  $\Xi$  has rank  $\leq 1$ , but otherwise, we have complete freedom over  $\Xi$  with respect to  $\tilde{T}$ . Thus, it is necessary and sufficient for the rows of  $Q$  to be linearly independent and to each satisfy  $\text{rk}(Q_{i,:} \times_0 \tilde{T}) \leq 1$  for all  $i$ . We can find such a set of rows by extracting a basis subset of  $S := \{v \in \mathbb{F}^{1 \times n_0} : \text{rk}(v \times_0 \tilde{T}) \leq 1\}$  using Gaussian elimination, or determining that such a basis does not exist.

If we do find a satisfying  $Q$ , then by Lemma 1 we can find a rank- $\leq 1$  CPD of each  $Q_i \times_0 \tilde{T}$  in polynomial time; join these CPDs and transform the first factor matrix by  $Q^{-1}$  to create a rank- $\leq R$  CPD of  $\Xi$ ; and join with  $((A_0)_{:,n_0}, \dots, (A_{D-1})_{:,n_0})$  to create a rank- $\leq R$  CPD of  $T$ . All that remains is to enumerate all possible tensors  $\tilde{T}$ , which can be done by enumerating  $((A_0)_{:,n_0}, \dots, (A_{D-1})_{:,n_0})$ .

### 3.2 Complexity

There are  $|\mathbb{F}|^{(R-n_0)(\sum_d n_d)}$  many possible assignments of  $((A_0)_{:,n_0}, \dots, (A_{D-1})_{:,n_0})$  to fix, and thus that many  $\tilde{T}$  to iterate over. For each  $\tilde{T}$  when we solve for  $Q$ : enumerating each  $v$  takes  $|\mathbb{F}|^{n_0}$  time; checking  $\text{rk}(v \times_0 \tilde{T}) \leq 1$  takes polynomial time by Lemma 1; and

$$\dim(\text{span}\{S\}) = \text{rk} \begin{pmatrix} \vdots \\ v \\ \vdots \end{pmatrix}_{v \in S}$$

time using Gaussian elimination. Thus, this subroutine takes  $O^*(|\mathbb{F}|^{n_0})$  time.

Overall, our algorithm runs in time  $O^*(|\mathbb{F}|^{(R-n_0)(\sum_d n_d + n_0)})$ . We can improve this time complexity by permuting the axes of  $T$  so that  $n_0$  is the longest shape length of  $T$ , allowing us to replace  $n_0$  in the expression with  $n_* := \max_d n_d$ .

The pseudocode for this algorithm is shown in Algorithm 1, which is implemented to consume polynomial space. One can modify the algorithm to more closely resemble depth-first search, e.g., by fixing tuples of columns  $((A_0)_{:,r}, \dots, (A_{D-1})_{:,r})$  for each  $n_0 \leq r < R$  at a time.

## 4. Border Rank

### 4.1 Motivation and Definitions

Intuitively, a border CPD is a parameterized CPD that approximates a target tensor  $T$  arbitrarily well. Such a CPD may have a strictly smaller rank than  $\text{rk}(T)$ : a famous example is  $T = \begin{bmatrix} 0 & 1 \\ 1 & 0 \end{bmatrix} \begin{bmatrix} 1 & 0 \\ 0 & 0 \end{bmatrix}$ , which has rank 3 but is approximated by the rank-2 border CPD  $\frac{1}{x} \left( \begin{bmatrix} 1 \\ x \end{bmatrix}^{\otimes 3} - \begin{bmatrix} 1 \\ 0 \end{bmatrix}^{\otimes 3} \right)$  as  $x \rightarrow 0$ .

To formally define border CPDs, we multiply everything by a high enough power of  $x$  so that everything is a polynomial in  $x$ . Define the following for a tensor with elements in  $\mathbb{F}$  (Bläser, 2013):

- $\underline{\text{rk}}_H(T) := \text{rk}(x^{H-1}T)$  over the polynomial ring  $\mathbb{F}[x]/(x^H)$ ; we call  $H$  the *exponent threshold*.
- $\underline{\text{rk}}(T) := \min_{H \geq 1} \underline{\text{rk}}_H(T)$ ; this is the border rank of  $T$ .

Border rank is useful in fast MM because one can essentially pretend it is regular rank for time complexity purposes. Recall from the introduction that finding a rank- $R$  CPD of the  $\mathcal{M}_{(m,k,n)}$  tensor leads to a  $O(N^{3 \log_{mn} R})$ -time algorithm for multiplying two  $N \times N$  matrices; it turns out this is also true for a border rank- $R$  CPD (with arbitrary exponent threshold  $H$ ), up to an extra  $O(N^\epsilon)$ -factor in the running time for arbitrarily small  $\epsilon > 0$  (Bläser, 2013). Because border rank allows extra freedom over regular tensor rank, due to multiples of  $x^H$  vanishing, most tensors (including MM tensors) usually have border CPDs with strictly lower rank than their tensor rank, making it easier to develop asymptotically fast algorithms for MM.

### 4.2 Border depth-first search

To make the search problem finite, we fix the exponent threshold  $H$ . We also generalize the problem to finding the CPD rank of a tensor with elements in the ring  $\mathcal{R} := \mathbb{F}[x]/(x^H)$ , i.e., elements are not restricted to  $\mathbb{F}$ -multiples of  $x^{H-1}$ . We call  $R$  the *border ring on field  $\mathbb{F}$  with exponent threshold  $H$* .

We can use the same depth-first search algorithm described in Section 2 to search for border CPDs; all we need is an efficient border analog of axis-reduction. It suffices to generalize *matrix rank factorization* to border rings:

Given  $M \in \mathcal{R}^{m \times n}$ , find  $U \in \mathcal{R}^{m \times r}$ ,  $V \in \mathcal{R}^{r \times n}$  such that  $M = UV$  and  $r$  is minimized.

Before proceeding, we use the following lemma about multiplicative inverses:

**Lemma 2.** *An element  $\alpha \in \mathbb{F}[x]/(x^H)$  has a multiplicative inverse if and only if it is not a multiple of  $x$ . Furthermore, such an inverse is unique and can be found in  $O(H^2)$  time.*

**Proof.** Clearly, if  $\alpha$  is a multiple of  $x$  it cannot have a multiplicative inverse because 1 is not a multiple of  $x$ . Otherwise,  $\alpha = \sum_{0 \leq h < H} \alpha_h x^h$  for  $\alpha_h \in \mathbb{F}$  and  $\alpha_0 \neq 0$ . Suppose  $\beta := \sum_{0 \leq h < H} \beta_h x^h$ ,  $\beta_h \in \mathbb{F}$  satisfies  $\alpha\beta = 1$ .

Then  $\beta_0 = \frac{1}{\alpha_0}$  and  $\forall h \geq 1: \beta_h = -\frac{1}{\alpha_0} (\sum_{h' < h} \alpha_{h-h'} \beta_{h'})$ .

We sketch the following procedure for row-reduction on  $M$ :

- Initialize a row index  $r < 0$ .
- Find an invertible element of  $M$ ; move it to row  $r$  using a row swap, normalize the row, and denote this as a pivot; then eliminate all other elements in the same column as the pivot and increment  $r$ .
- Repeat this process, but now with the first row frozen, i.e., it cannot be modified or moved.
- If at some point we cannot find an invertible element, we instead try to find an element of the form  $x\gamma$  for invertible  $\gamma$ , normalize it to  $x$ , and then only eliminate terms that are multiples of  $x$ ; if we cannot find such an element, repeat for  $x^2\gamma$ , and so on.
- At the end, remove any all-zeros rows and set  $V$  to this matrix.
- Throughout this entire process, update  $U$  as we perform each row operation; at the end, keep only its leftmost  $r$  columns.

$V$  will have a form similar to row echelon form (not necessarily *reduced* row echelon form), up to permutation of columns, except that the leading terms are powers of  $x$ .

To prove that such  $V$  has the minimum number of rows for matrix rank factorization, we first simplify it further with column operations. For each leading term  $x^h$ , all other elements on the same row must be multiples of  $x^h$  because we could have only had  $x^h$  as a leading term if the non-frozen rows had no more terms  $x^h \gamma$  for  $h' < h$  and invertible  $\gamma$ . This property means that  $V$  can be reduced to the form  $\begin{bmatrix} I_{b_0} & & \\ & \ddots & \\ & & x^{H-1} I_{b_{H-1}} \end{bmatrix}$  using column operations, up to the presence

of extra all-zeros columns.

We now prove that the rank of this reduced matrix is equal to the number of nonzeros on its diagonal (Conner, 2024):

**Lemma 3.** *Over  $\mathbb{F}[x]/(x^H)$ ,  $\text{rk}(x^h I_n) = n$  for all  $h < H$ .*

---

**Algorithm 1** Search algorithm for rank- $\leq R$  CPD over a finite field  $\mathbb{F}$ 


---

**Precondition:**  $T \in \mathbb{F}^{r_0 \times \dots \times r_{D-1}}$ ,  $T$  axis-reduced,  $R \in \mathbb{Z}_{\geq 0}$ **Postcondition:** returns a rank- $\leq R$  CPD of  $T$ , if one exists; else, returns null

```

1: function RREF_SEARCH_HELP( $T, R$ )
2:   for  $0 \leq d' < D$ ,  $V_{d'} \in \mathbb{F}^{r_{d'} \times (R-r_0)}$  do
3:      $\tilde{T} \leftarrow T - \llbracket V_0, \dots, V_{D-1} \rrbracket$ 
4:     for  $0 \leq d < D$  do
5:        $U_d \leftarrow []$ 
6:      $Q \leftarrow []$ 
7:      $x \leftarrow 0$ 
8:     for  $v \in \mathbb{F}^{1 \times r_0}$  do
9:        $t, u_1, \dots, u_{D-1}, s_1, \dots, s_{D-1} \leftarrow \text{AXIS\_REDUCE}((v \times_0 T)_{0, \dots, \dots})$ 
10:      if  $(\forall d > 1 : s_d \leq 1)$  and  $\text{rk} \left( \begin{bmatrix} Q \\ v \end{bmatrix} \right) > \text{rk}(Q)$  then
11:         $Q \leftarrow \begin{bmatrix} Q \\ v \end{bmatrix}$ 
12:        if  $\forall d > 1 : s_d > 0$  then
13:           $u_0 \leftarrow t_{0, \dots, 0} e_x \triangleright e_x$  is the  $n_0$ -long vector with a 1 at index  $x$  and 0s everywhere else
14:          for  $0 \leq d < D$  do
15:             $U_d \leftarrow [ U_d \mid u_d ]$ 
16:           $x \leftarrow x + 1$ 
17:          if  $x = n_0$  then
18:            return  $(Q^{-1} [ U_0 \mid V_0 ], [ U_1 \mid V_1 ], \dots, [ U_{D-1} \mid V_{D-1} ])$ 
19:      return null

```

**Precondition:**  $T_{\text{target}} \in \mathbb{F}^{n_0 \times \dots \times n_{D-1}}$ ,  $R \in \mathbb{Z}_{\geq 0}$ **Postcondition:** returns a rank- $\leq R$  CPD of  $T_{\text{target}}$ , if one exists; else, returns null

```

20: function RREF_SEARCH( $T_{\text{target}}, R$ )
21:    $T, Q_0, \dots, Q_{D-1}, r_0, \dots, r_{D-1} \leftarrow \text{AXIS\_REDUCE}(T_{\text{target}})$ 
22:   if  $\exists d | r_d > R$  then
23:     return null
24:   if  $\exists d | r_d = 0$  then
25:     return  $([])_{0 \leq d < D}$ 
26:    $d^* \leftarrow \arg \max_d r_d$ 
27:    $A \leftarrow \text{RREF\_SEARCH\_HELP}(\llbracket T_{i_0, \dots, i_{D-1}} \rrbracket_{i_{d^*}, i_1, \dots, i_{d^*-1}, i_0, i_{d^*+1}, \dots, i_{D-1}}, R) \triangleright$  swap axes 0 and  $d^*$ 
28:   if  $A \neq \text{null}$  then
29:     for  $0 \leq d < D$  do
30:        $U_d \leftarrow (Q_d^{-1})_{:, r_d} A_d$ 
31:     return  $(U_{d^*}, U_1, \dots, U_{d^*-1}, U_0, U_{d^*+1}, \dots, U_{D-1})$ 
32:   return null

```

---

*Proof.* Suppose there was a rank- $< n$  CPD of  $x^h I_n = \llbracket A_0, A_1 \rrbracket = A_0 A_1^\top$ . If we compute this CPD over the larger polynomial ring  $\mathbb{F}[x]$ , then  $A_0 A_1^\top = x^h I_n + x^H X$  for some arbitrary  $X \in \mathbb{F}[x]^{n \times n}$ .

We have  $\det(A_0 A_1^\top) = 0$ , since row-reducing  $A_0$  is guaranteed to yield at least one row of all zeros (due to having fewer columns than rows), so there exists a sequence of row operations on  $A_0 A_1^\top$  that also produces an all-zeros row.

However,  $\det(x^h I_n + x^H X) = x^{hn} + o(x^{hn})$  where  $o(x^p)$  hides terms containing  $x$  raised to a power  $> p$ ; this is because in the Leibniz formula of the determinant, the term corresponding to the main diagonal is  $x^{hn}$ , whereas all other terms have  $x$  raised to a strictly higher power. Hence, a contradiction.

**Lemma 4.** Over  $\mathbb{F}[x]/(x^H)$ , let  $N := \begin{bmatrix} I_{b_0} & & \\ & \ddots & \\ & & x^{H-1} I_{b_{H-1}} \end{bmatrix}$ ; then  $\text{rk}(N) = \sum_n b_n$ .

*Proof.* Clearly  $\text{rk}(N) \leq \sum_n b_n$ . To show the lower bound, multiply each  $x^h I_{b_h}$  block by  $x^{H-1-h}$  so that all terms on the diagonal are  $x^{H-1-h}$ ;

doing so cannot increase the rank. Then by Lemma 3, this matrix has rank  $\sum_n b_n$ .

Pseudocode for border CPD search is provided in Algorithm 2. To bound its running time, note that a call will only recurse if all axis-ranks  $r_d$  are  $\leq R$ ; if so, it branches to  $|\mathbb{F}|^H \sum_d r_d$  children that each replace the parameter  $R$  with  $R - 1$ . Thus, if we now define  $r_d$  to be the axis- $d$  rank of the original target tensor  $T$ , the total running time is  $O^*(|\mathbb{F}|^H \sum_{1 \leq r \leq R} \sum_d \min(r, r_d))$ .

## 5. Conclusion and Next Steps

We have presented an  $O^*(|\mathbb{F}|^{(R-\max_d n_d)(\sum_d n_d) + \max_d n_d})$ -time algorithm for finding a rank- $\leq R$  CPD (or proving such a CPD does not exist) of a tensor with shape  $n_0 \times \dots \times n_{D-1}$  and elements in a finite field  $\mathbb{F}$ , as well as a  $O^*(|\mathbb{F}|^H \sum_{1 \leq r \leq R} \sum_d \min(r, n_d))$ -time algorithm to solve the same problem for a tensor with elements in the ring  $\mathbb{F}[x]/(x^H)$ . Both algorithms are substantially faster than brute force, with an important reason why being axis-reduction; both algorithms also use polynomial space.

**Algorithm 2** Depth-first search algorithm for rank- $\leq R$  CPD over border ring  $\mathbb{F}[x]/(x^H)$

**Precondition:**  $T_{\text{target}} \in (\mathbb{F}[x]/(x^H))^{n_0 \times \dots \times n_{D-1}}$ ,  $R \in \mathbb{Z}_{\geq 0}$

**Postcondition:** returns a rank- $\leq R$  CPD of  $T_{\text{target}}$ , if one exists; else, returns null

```

1: function DFS( $T_{\text{target}}, R$ )
2:    $T, Q_0, \dots, Q_{D-1}, r_0, \dots, r_{D-1} \leftarrow \text{BORDER\_AXIS\_REDUCE}(T_{\text{target}})$ 
3:   if  $\exists d | r_d > R$  then
4:     return null
5:   if  $\exists d | r_d = 0$  then
6:     return  $([])_{0 \leq d < D}$ 
7:   for  $0 \leq d < D$ ,  $u_d \in (\mathbb{F}[x]/(x^H))^{r_d}$  do
8:      $A \leftarrow \text{DFS}(T - \otimes_d u_d, R - 1)$ 
9:     if  $A \neq \text{null}$  then
10:      return  $((Q_d^{-1})_{:,r_d} [ A_d \mid u_d ])$ 
11:   return null

```

There is a large gap between the time complexity for border CPD and what it could be if our algorithm for exact CPD generalized to the border analog. The main issue is that reduced row-echelon form does not always exist over  $\mathbb{F}[x]/(x^H)$  (where we are only allowed row operations) because a leading term that is not equal to 1 may have elements above it that are not multiples of itself; an example is  $\begin{bmatrix} 1 & 1 \\ & x \end{bmatrix}$  for  $H \geq 2$ . A corollary is that a full-rank square

matrix is not necessarily invertible over border rings, in stark contrast to fields.

One possible way to close this gap is to analyze what happens when  $R = \max_d r_d$ , where  $r_d$  is the axis- $d$  rank of the original target tensor. In this situation, we suspect that only  $o(|\mathbb{F}|^{H \sum_d r_d})$  many children of the root call in Algorithm 2 will recurse into their own children, because most children calls fail to reduce any axis-ranks of the target tensor. Studying this problem further could result in tighter time bounds without changing the algorithm.

**Acknowledgments**

We thank Prof. Virginia Vassilevska Williams for her continual mentorship throughout the years on this research topic, and Austin Conner for resolving how to calculate the rank of a general matrix over a border ring. We also thank Prof. Erik Demaine and Ani Sridhar for motivating us to pivot our research from fast matrix multiplication tensors to general tensors.

**References**

Alman, Josh and Hengjie, Zhang. (2023). Generalizations of Matrix Multiplication can solve the Light Bulb Problem. Retrieved on Oct 4, 2024 from <https://arxiv.org/abs/2311.01630>

Alman, Josh and Turok, Ethan and Yu, Hantao and Zhang, Hengzhi. (2024). Tensor Ranks and the FineGrained Complexity of Dynamic Programming. Retrieved on Oct 4, 2024 from <https://arxiv.org/abs/2309.04683>

Bläser, Markus. (2013). Fast Matrix Multiplication. Theory of Computing, 5. Retrieved on Oct 4, 2024 from <https://theoryofcomputing.org/articles/gs005/>

Chan, Timothy M. (2022). Finding Triangles and Other Small Subgraphs in Geometric Intersection Graphs. Retrieved on Oct 4, 2024 from <https://arxiv.org/abs/2211.05345>

Conner, Austin. (2024). Retrieved on Oct 4, 2024 from private communication.

Courtois, Nicolas T. and Bard, Gregory V. and Hulme, Daniel. (2011). A New General-Purpose Method to Multiply 3x3 Matrices Using Only 23 Multiplications. Retrieved on Oct 4, 2024 from <https://arxiv.org/abs/1108.2830>

Fawzi, Alhoussein and Balog, Matej and Huang, Aja and Hubert, Thomas and Romera-Paredes, Bernardino and Barekatin, Mohammadamin and Novikov, Alexander and Ruiz, Francisco J. R. and Schrittwieser,

Julian and Swirszcz, Grzegorz and Silver, David and Hassabis, Demis and Kohli, Pushmeet. (2022). Discovering faster matrix multiplication algorithms with reinforcement learning. Nature, 610, 47–53. Retrieved on Oct 4, 2024 from <https://www.nature.com/articles/s41586-022-05172-4>

Heule, Marijn J.H. and Kauers, Manuel and Seidl, Martina. Local Search for Fast Matrix Multiplication. Retrieved on Oct 4, 2024 from <https://arxiv.org/abs/1903.11391>

Håstad, John. (1990). Journal of Algorithms, 11, 644-654. Retrieved on Oct 4, 2024 from [https://doi.org/10.1016/0196-6774\(90\)90014-6](https://doi.org/10.1016/0196-6774(90)90014-6)

Kauers, Manuel and Moosbauer, Jakob. (2022). Flip Graphs for Matrix Multiplication. Retrieved on Oct 4, 2024 from <https://arxiv.org/abs/2212.01175>

Shitov, Yaroslav. (2016). How hard is the tensor rank?. Retrieved on Oct 4, 2024 from <https://arxiv.org/abs/1611.01559>

# Deep-Sea Sediment Sampler for Hadal Depths

Audrey Chen<sup>1</sup>, Jessica Lam<sup>1</sup>, Thao Do<sup>1</sup>, Ansel J Garcia-Langley<sup>1</sup>, Ved Ganesh<sup>1</sup>, Andrew Bennett<sup>2</sup>, Michael Triantafyllou<sup>3</sup>

<sup>1</sup> Student Contributor, MIT Class of 2021, MIT Sea Grant & MIT Department of Mechanical Engineering, Cambridge, MA 02139

<sup>2</sup> Supervisor, Department of Earth, Atmospheric and Planetary Sciences, Cambridge, MA 02139

<sup>3</sup> Supervisor, Department of Earth, Atmospheric and Planetary Sciences, Cambridge, MA 02139

**SEDIMENT CORES ARE GATHERED TO COLLECT DATA ON SEABED CHEMICAL AND MINERAL COMPOSITION. THIS PAPER REVIEWS THE PROCESS OF DESIGNING AND TESTING A PURELY MECHANICAL SEDIMENT SAMPLER FOR USE AT HADAL DEPTHS. THESE SAMPLES ARE IMPORTANT IN DETERMINING THE HEALTH OF THE SURROUNDING ENVIRONMENT AND GIVE US INSIGHT INTO WHAT ORGANISMS CURRENTLY LIVE OR HAVE LIVED ON OR IN THE SEABED. SEDIMENT SAMPLES ARE RELEVANT TO MANY FIELDS OF RESEARCH, INCLUDING MARINE ARCHAEOLOGY, BIOLOGY, ECOLOGY, GEOLOGY, AND CLIMATE SCIENCE. OVER THE LAST FEW DECADES, LIMITED MISSIONS TO COLLECT SEDIMENT CORE SAMPLES HAVE BEEN MADE FROM AS DEEP AS THE MARIANA TRENCH, WHICH CONTAINS THE DEEPEST KNOWN POINT ON EARTH'S SURFACE AT 11,000 METERS (DAI, XU, & CHEN, 2021; WANG, 2022). THE ENVIRONMENTAL HISTORY AND TRAJECTORY OF OUR OCEAN FLOORS ARE NOT WELL UNDERSTOOD, AND DEEP SEA SEDIMENT CORES ARE CRUCIAL IN FILLING THIS GAP.**

**WORKING IN CONJUNCTION WITH INKFISH, A SUBMERSIBLE TECHNOLOGY COMPANY, WE DEVELOPED A DEEP-SEA SEDIMENT CORE SAMPLER THAT WILL TRAVEL TO THE MARIANA TRENCH ABOARD ONE OF INKFISH'S SUBMERSIBLE LANDERS AND WILL COLLECT FOUR INCHES OF SEDIMENT AT AMBIENT PRESSURES OF 110.32 MPA (NATIONAL OCEANIC AND ATMOSPHERIC ADMINISTRATION, 2016). OUR SEDIMENT SAMPLING PROTOTYPE HAD TO FULFILL SEVERAL DESIGN REQUIREMENTS THAT RESULTED FROM ENVIRONMENTAL CONDITIONS, LANDER CONSTRAINTS, AND SAMPLE CONDITION SPECIFICATIONS. WE DESIGNED AN ENTIRELY MECHANICAL SAMPLER BECAUSE UNDERWATER ACTUATORS SUITABLE FOR USE IN HADAL CONDITIONS ARE DIFFICULT TO SOURCE AND REQUIRE ADDITIONAL COMMUNICATION AND POWER RESOURCES. THE EXTREME PRESSURE IN THE MARIANA TRENCH IMPOSED RESTRICTIONS ON THE MATERIALS WE COULD USE AND LED OUR DESIGN TO INCORPORATE LOW-PRECISION INTERFACES. ADDITIONALLY, THE SEDIMENT CORE SAMPLING SYSTEM IS LIMITED IN SIZE AND WEIGHT TO AVOID INTERFERING WITH THE FUNCTIONALITY OF UNCREWED SEAFLOOR LANDERS. MOST IMPORTANTLY, THE LAYERS OF THE SEDIMENT CORE SAMPLES MUST BE PRESERVED AND SECURED AS THE LANDER ASCENDS TO PRESERVE RELATIVE TIME SCALES WITHIN THE SAMPLE. OUR PURELY MECHANICAL SEDIMENT COLLECTION SYSTEM CONSISTS OF THE COLLECTION TUBE SUBSYSTEM, WHICH IS RESPONSIBLE FOR COLLECTING AND RETAINING THE SEDIMENT, AND THE SAMPLING FRAME SUBSYSTEM, WHICH AIMS TO FACILITATE THE INSERTION AND RETRACTION OF THE TUBE FROM THE SEAFLOOR. IN ORDER TO MEET THE PARTICULAR LOADING AND UNLOADING CONSTRAINTS OF INKFISH'S SEAFLOOR LANDERS, WE ALSO DEVELOPED A DEPLOYMENT MECHANISM THAT ENSURES THE LANDER IS FULLY CONTAINED WITHIN THE PAYLOAD BAY IN ITS PRIMED STAGE AT THE START OF THE OPERATION AND ONCE AGAIN AT THE END OF THE OPERATION. OUR GOAL FOR THIS ITERATION WAS TO DETERMINE THE VALIDITY OF THE COLLECTION AND RETENTION METHODS, WHICH ARE DRIVEN BY THE CONSTRAINTS OF THE ENVIRONMENT AT HADAL DEPTHS. STILL, THE MATERIALS AND MANUFACTURING METHODS FOR THIS VERSION ARE NOT SUFFICIENT TO SURVIVE THE EXTREME HADAL ENVIRONMENT. IF TESTING IS SUCCESSFUL, ANOTHER UNIT WILL BE DEVELOPED TO BE DEPLOYED AT 11,000 M.**

**ULTIMATELY, OUR SEDIMENT SAMPLER PRESENTS A VIABLE PURELY MECHANICAL SOLUTION TO COLLECTING DEEP-SEA SEDIMENT FROM UNEXPLORED AREAS AT HADAL DEPTHS LIKE THE MARIANA TRENCH. OUR SAMPLER CAN EASILY BE MOUNTED ONTO ANY SURFACE WHERE IT WOULD TOUCH THE OCEAN FLOOR, REQUIRING NO ELECTRONICS OR CONTROLS. THOUGH WE WERE CONSTRAINED BY THE PARTICULAR SEAFLOOR LANDER USED BY INKFISH, THE SIZE OF THE SAMPLER IS SCALABLE, ALLOWING BOTH THE SAMPLE DIAMETER AND DEPTH TO BE ADJUSTED FOR A GIVEN MISSION. BY MAKING THESE SEDIMENT SAMPLES MORE ACCESSIBLE, WE BELIEVE WE WILL HAVE AN IMPACT ON A NUMBER OF MARINE RESEARCH AREAS.**

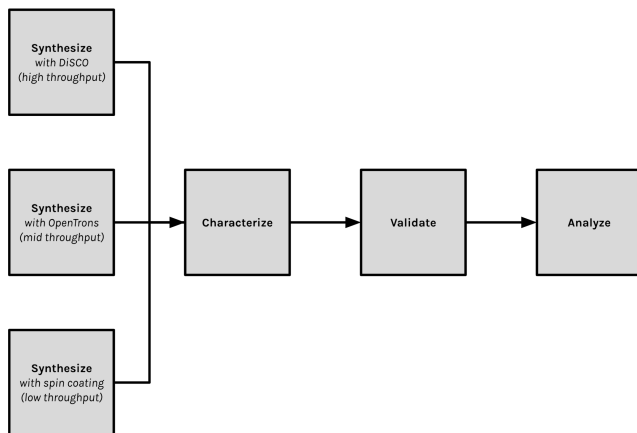
### 1. Background

The environment near the aquatic floor is one of the most biodiverse areas in the ocean ecosystem, relying on sediment for nutrients and shelter (NSF NEON, 2024). Scientists assess ecosystem health by analyzing sediment core samples, which preserve layers of sediment and offer insights into environmental history. These samples are collected from a range of benthic ecosystems, including the hadal zone—depths of 6,000 to 11,000 meters—where extreme conditions pose significant technological challenges.

Current samplers are large, complex, and resource-intensive, limiting accessibility. For example, in 2006, a gravity-type core sediment sampler named “Asyura” was deployed to the deepest part of the Mariana Trench, the Challenger Deep, and successfully collected a sediment core (IEEE, 2024). Similarly, a novel pressure-retaining sampler was also deployed to the Challenger Deep in 2021 and was also able to successfully collect a sediment sample (Wang, 2022). However, the technology used for these expeditions is large, complex, and/or heavy. The “Asyura” system weighed 100 kg in air and occupied 75x75x107 cm<sup>3</sup>. The pressure-retaining sampler weighed 65 kg in air and utilized motors and onboard computing. Additionally, many of these devices require a dedicated vehicle for the expedition, whether a submersible, ROV, or lander. “Asyura,” for example, was deployed using an ROV and two cables that stretched the 11,000 m distance from the surface to the Challenger Deep. As a result, these devices are not particularly accessible to organizations that are unable to dedicate such resources and funding to sediment sampling.

In collaboration with Inkfish, we are developing a lightweight, mechanical sediment corer that can be easily attached to landers, enhancing the accessibility of sediment core sampling in hadal environments.

### 2. Design



Our sediment sampler device is designed to work in conjunction with an Inkfish lander, which introduces certain design constraints. The landers have little to no onboard computation and an extremely

limited available power supply of 48V DC. Additionally, our device must fit within one of the lander’s bays, which has roughly 50x60x100 cm<sup>3</sup> of space and a 40x50 cm<sup>2</sup> opening to access the seafloor. The landers are raised and lowered into the water by crane from the research vessel, and as such, the sampling device must always remain within the confines of the seafloor lander during crane operation. Our device must also weigh less than 10 kg in water (roughly 15.8 kg in air) to avoid interfering with the lander’s ability to resurface. This prototype is intended to be deployed at a depth of 3,000 m and test the collection and retention method and deployment mechanisms. If testing is successful, a new version will be developed to withstand the extreme hadal conditions.

A deployment mechanism houses the sediment sampling system and connects it to the seafloor lander. This mechanism holds the primed sampling system with its extended base plate up in the lander bay during initial crane operation. Once the lander is deployed in the ocean, a set of timed water-soluble fasteners dissolve, which allows a spring-loaded elbow latch to lower the entire sampling rig down into position with the base plate protruding beneath the lander. Once it slides down into its lower position along a set of stainless steel slides, it locks into place and remains at that height for the rest of the operation, as seen in

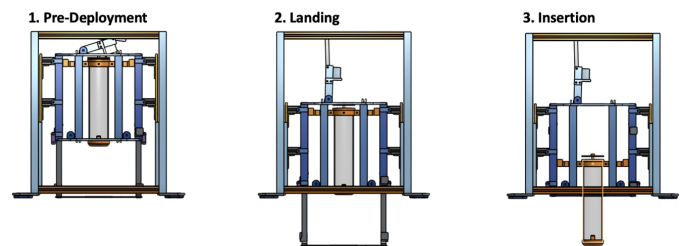


Figure 2. The three stages of deployment. Water-soluble fasteners and spring not pictured.

Figure 2.

As seen in Figure 3, there are three stages to the sediment collection process once the lander nears the seafloor. In the first stage, the base plate lands and settles against the seafloor. In the second stage, the lander continues to sink down until it also makes contact with the seafloor. The weight of the lander and the force of the seafloor upwards act on the base plate to trigger a spring-pulley system that inserts the collection tube into the sediment. In the third and final stage, the tube is retracted from the sediment, and the base plate reaches its final position within the lander’s bay.

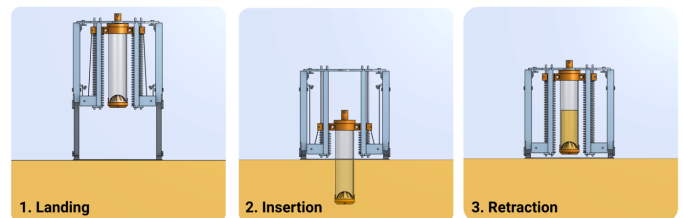


Figure 3. The three stages of the sediment collection process of our mechanical deep-sea sediment sampler device: landing, insertion, and retraction.

The sediment core sampling device consists of two main subsystems: the frame and the collection tube. The collection tube collects and retains the sediment while the frame inserts and retracts the tube from the seafloor without the use of any electrical components.

The collection tube captures sediment once the lander has reached the seafloor and secures the sediment until the lander is collected from the ocean. The sediment should be able to enter the tube without much difficulty in order to minimize the disturbance to the top layers of the seafloor. The ascension from the bottom of the Mariana Trench to the surface is estimated to take roughly four hours, and the lander will spend between 30 minutes to an hour bobbing at the surface of the water before it is recovered. The collection tube must be robust and secure enough to be able to retain the sediment sample throughout this process.

At the top of the tube is an aluminum cap that allows the tube to be connected to the spring-pulley system. Furthermore, the top of the cap functions as a one-way valve that allows water to escape as sediment is collected within the tube. The valve also creates a pressure seal that helps prevent sediment from escaping. We explored two potential valves: a spring-loaded ball valve and a rubber flap valve (Figure 4).

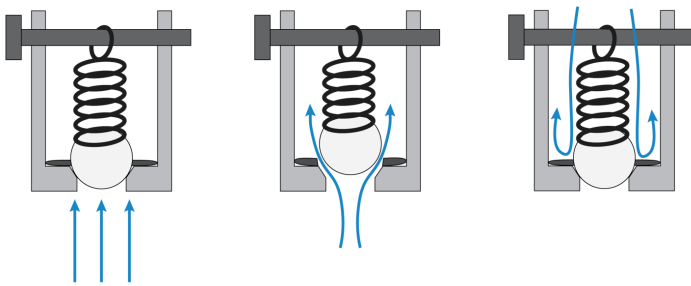


Figure 4. Stages of spring-loaded ball valve during sediment collection

For the ball valve, the spring and o-ring create a strong seal that prevents water from entering from the top of the tube during ascension and driving out the collected sediment. The valve requires roughly 2 lbs of force to operate and has a 1.82 cm<sup>2</sup> opening for water to escape.

Alternatively, the rubber flap valve is a simpler system that utilizes the movement of the lander to drive the valve. During descent and as the tube is driven into the sediment, the rubber flap slides up the center shaft and exposes the holes at the top of the cap, allowing water to escape through the 7.07 cm<sup>2</sup> of available space. The upward motion during the retraction of the tube and ascension to the surface pulls the rubber down the shaft. The rubber presses against the holes, deforms, and creates a seal.

At the bottom of the collection tube is a nose cone that helps dig into sediment. The nose cone is fabricated from Markforged Onyx, which is less brittle than the polycarbonate tube and helps prevent the fracturing of the tube if the lander encounters rocky terrain. The nose cone also serves as the component that secures the sediment collection apparatus to the collection tube. There are two collection apparatuses considered: a core catcher and a rubber mud flap.

The core catcher apparatus (Figure 5) is simple in design and consists of only a plastic hollow demi-sphere-shaped component. The hollow demi-sphere shape is formed by a ring of slightly triangular-shaped fingers that are pushed open by entering sediment and closed upon retraction from the upward motion of the tube paired with the weight of the sediment. This design results in sediment layers mixing at the edges of the core sample, but we hypothesize that sediment layers at the center of the sample will be preserved.

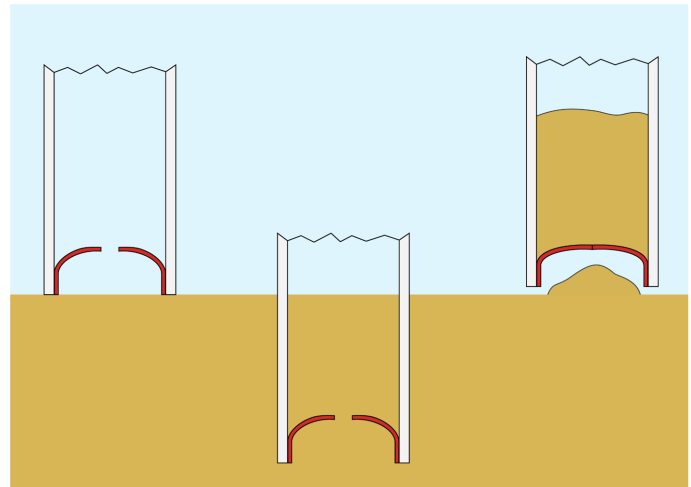


Figure 5. Stages of core catcher apparatus during sediment collection.

The rubber mud flap (Figure 6) consists of a circular rubber flap, an aluminum shaft, steel loop clamps, and a unique onyx nose cone. The rubber flap is secured onto the aluminum shaft using loop clamps. When the tube is inserted into the sediment, the rubber flap deforms, allowing sediment to enter. The nose cone for the rubber mud flap has a lip that protrudes into the tube. This lip, paired with the circular rubber flap, creates a seal that prevents sediment and water from escaping during retraction and ascension. However, since the mud flap only allows the sediment to enter through one side, the stratification of the sediment layers is unlikely to be preserved.

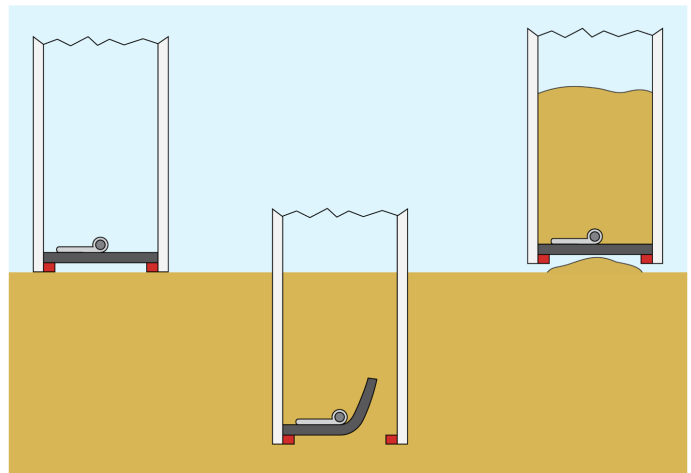


Figure 6. Stages of rubber mud flap apparatus during sediment collection.

The frame subsystem, responsible for driving the collection tube into and removing from the sediment, can be further separated into a static segment and a dynamic segment. The static segment (Figure 7, left) is permanently fixed relative to the lander and primarily provides structural support and stiffness to allow the dynamic segment to actuate sediment collection. The top plate, two rod plates, and the two box tube extrusions act as the foundation of the static segment and provide the majority of the stiffness. Furthermore, four aluminum bars between the two plates supply additional stiffness and act as rails to prevent the cap of the tube from sliding or bending. Similarly, the six fixed aluminum rods prevent the springs from shifting or buckling during compression.



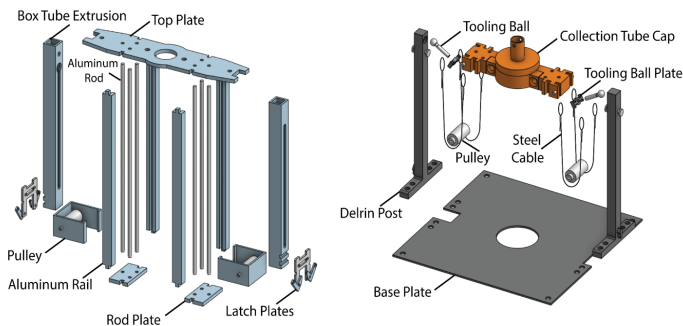


Figure 7. Components of the static segment of the frame subsystem (left) and components of the dynamic segment of the frame subsystem (right).

In addition to providing stiffness, the static segment also provides support to the dynamic segment (seen on the right in Figure 7). The two pulleys of the spring-pulley system are permanently fixed between the rails and the box tubes. Additionally, there is a spring-driven latch system attached to the box tubes that ensures that the base plate of the dynamic system is safely enclosed within the bay of the lander before ascending.

The dynamic segment is the core of the purely mechanical sediment collection system. The dynamic segment consists of a base plate with two Delrin posts fastened to the plate. At the top of each post is a pocket where a tooling ball sits. Each of the four steel cables is looped around a pulley. One end of the cable is fixed around an arm of a tooling ball plate, while the other end is connected to a rod at the side of the collection tube cap.

At the core of the frame is a spring-pulley mechanism that utilizes the change in distance of the base plate relative to the lander as a trigger to push the collection tube into the sediment. Before reaching the seafloor, the base plate is positioned below the bottom of the lander. Once the base plate makes contact with the ground, the upward force from the base plate-ground interaction and the downward force from the weight of the lander result in the two box tubes sliding down the two posts. As the posts travel up the box tubes, the cap of the collection tube is pulled down, and the two springs are compressed. The posts slide until they travel the maximum length, roughly 159 mm, at which point the tooling balls are pulled out of the posts due to the tension from the steel cable. With the tension released, the springs are then able to decompress and push the cap of the tube up.

In order for the sediment sampler device to perform reliably, most of the components are made of aluminum due to its minimal volumetric strain under maximum hadal pressures (less than 3%). All aluminum pieces were coated with polytetrafluoroethylene (PTFE) during anodization to reduce sliding friction and enhance the system's structural strength. Furthermore, all systems, such as the sliding, pulley, and latch systems, have low-precision interfaces. Thus, material compression under extreme pressures would not result in diminished performance but may even induce increased efficiency.

### 3. Testing and Validation

We conducted field testing to evaluate the sediment collection and retention capabilities of our apparatuses and one-way valves. The sediment collection tube was attached to a five-meter pole, manually inserted and retracted from the Charles River bed at a depth of three meters. We tested each collection apparatus (rubber

mud flap and core catcher) with three valve configurations: no valve, a spring-ball valve, and a rubber flap valve. Three samples were collected for each combination.

	Core Catcher			Rubber Mud Flap														
	No Valve	Ball Valve	Rubber Flap Valve	No Valve	Ball Valve	Rubber Flap Valve												
Sediment Weight (g)	34.9	44.9	31.9	142.9	155.8	174.9	3.9	15.9	45.9	242.9	318.9	262.9	176.9	74.9	138.9	104.9	99.9	122.9
Water Weight (g)	484.9	278.9	294.9	542.9	796.8	903.8	554.9	644.8	915.8	760.8	636.8	708.8	942.8	858.8	737.8	862.8	736.8	845.8
Total Weight (g)	519.8	323.8	326.8	685.8	952.6	1078.7	558.8	660.7	961.7	1003.7	955.7	971.7	1119.7	933.7	876.7	967.7	836.7	968.7
Avg Total Weight (g)	390.1			905.7			727.1			977.0			976.7			924.4		
Avg S/W Ratio	0.114			0.217			0.027			0.397			0.154			0.134		

Table 1. Table of water and sediment weight for each sample collected using various combinations of sediment collection apparatuses and one-way valves.

The results showed that the rubber mud flap with no valve collected the most sediment and had the highest sediment-to-water ratio. The rubber mud flap combined with the ball valve came in a close second, indicating that this combination is nearly ideal for maximizing the total sample weight. Comparatively, the core catcher with a ball valve ranked lower in terms of sediment-to-water ratio, suggesting that the presence of a valve limits sediment collection due to the force needed to activate it.

Overall, the rubber mud flap apparatus consistently outperformed the core catcher in both sample weight and sediment-to-water ratio, regardless of valve configuration. While the ball valve did not outperform the no-valve setups, it performed better than the rubber flap valve, indicating that it is a viable option for applications where a valve is necessary.

### 4. Conclusion

In October, the sampler was shipped to Tonga for testing depths of 2,000 to 3,000 m. This test will assess the reliability and capabilities of our full system when mounted to a lander. Our device will be evaluated on a number of criteria, including the ease of attaching the device to the lander, the volume of sediment collected, and its reliability and robustness. We expect to hear back on the performance of the system by the end of 2024.

We believe that our purely mechanical sediment sampler offers a practical and efficient solution for collecting deep-sea sediment from unexplored regions at hadal depths, such as the Mariana Trench. If testing proves successful, our device will make deep-sea sediment sampling more accessible by enabling easy attachment to any seafloor contact point without the need for electronics or controls. Additionally, the design's scalability allows for adjustments in both sample diameter and depth, offering flexibility for different missions. By improving access to these valuable sediment samples, our system could have a significant impact across various marine research disciplines, from tracking pollutants (Kilic, 2023) to studying microbial diversity (Wang, 2022).

### 5. Future Work

Future work will focus on refining the sediment collection nozzles and optimizing the design based on the results from the upcoming Tonga tests. Field testing feedback will also guide modifications to enhance the system's performance on both seafloor landers deployed at hadal depths and in crewed submersible missions. Additionally, we aim to adapt the design for broader use in less extreme environments, expanding the

accessibility of sediment sampling. By further developing this purely mechanical system, we hope to support a variety of research fields, facilitating the collection of benthic sediment data in more diverse and cost-effective ways.

## References

[1] Dai, X., Xu, T., & Chen, J. (2021). Physical and mechanical properties of deep oceanic sediments cored from the bottom of Challenger Deep, Mariana Trench. *Geofluids*, 2021(1), 9109132. Retrieved on [insert date] from <https://doi.org/10.1155/2021/9109132>.

[2] Wang, H., et al. (2022). Collection of sediment from Mariana Trench with a novel pressure-retaining sampler. *Deep Sea Research Part Oceanographic Research Papers*, 183, 103740. Retrieved on [insert date] from <https://doi.org/10.1016/j.dsr.2022.103740>.

[3] National Oceanic and Atmospheric Administration. (2016, March 2). Seven miles deep, the ocean is still a noisy place. Retrieved on April 23, 2024, from <https://www.noaa.gov/media-release/seven-miles-deep-ocean-is-still-noisy-place>.

[4] National Science Foundation. (n.d.). Sediments — NSF NEON — Open Data to understand our ecosystems. Retrieved on July 28, 2024, from <https://www.neonscience.org/data-collection/sediments>.

[5] Kılıç, S., Kılıç, O., Belivermiş, M., & Ergül, H. A. (2023). Chronology of PAH and PCB pollution using sediment core in the Golden Horn estuary (Sea of Marmara). *Marine Pollution Bulletin*, 187, 114570. Retrieved on [insert date] from <https://doi.org/10.1016/j.marpolbul.2023.114570>.

[6] Sun, X., Song, X., Jiang, Z., Tang, Q., & Sun, Y. (2024). Biogenic silica in sediment core indicates the historical development of off-bottom oyster farming. *Science of The Total Environment*, 947, 174591. Retrieved on [insert date] from <https://doi.org/10.1016/j.scitotenv.2024.174591>.

[7] WorldAtlas. (n.d.). Ocean zones. Retrieved on August 1, 2024, from <https://www.worldatlas.com/oceans/ocean-zones.html>.

[8] Shank, T. (n.d.). The hadal zone: Aqua incognita. Retrieved on July 22, 2024, from <https://oceanexplorer.noaa.gov/oceanos/explorations/ex2102/features/hadalzone/hadalzone.html>.

[9] Jamieson, A. J., Fujii, T., Mayor, D. J., Solan, M., & Priede, I. G. (2010). Hadal trenches: The ecology of the deepest places on Earth. *Trends in Ecology & Evolution*, 25(3), 190–197. Retrieved on [insert date] from <https://doi.org/10.1016/j.tree.2009.09.009>.

[10] (n.d.). ECO Jan/Feb: Extreme exploration: The hadal zone. Retrieved on July 22, 2024, from <https://digital.ecomagazine.com/articles/extreme-exploration-the-hadal-zone>.

[11] “Sediment Sampling at a Depth of 10,131m in the Challenger Deep by ROV Kaiko.” (n.d.). Retrieved on July 31, 2024, from <https://ieeexplore-ieee-org.libproxy.mit.edu/document/4302339>.

[12] Caladan Oceanic. (2022, March 23). Deep Sea Planet. Retrieved on August 1, 2024, from <https://www.youtube.com/watch?v=lc8Ovo33fNc>.



THE SCIENCE *of* POSSIBILITY

**Vertex aims to create new possibilities in medicine to cure diseases and improve people's lives.**

We have some of the industry's best and brightest people helping us achieve our mission of discovering transformative medicines for people with serious diseases. The diversity and authenticity of our people is part of what makes us unique. By embracing our strengths and celebrating our differences, we inspire innovation together.

**For Internship Programs and Career Opportunities, visit [careers.vrtx.com](https://careers.vrtx.com)**

Vertex and the Vertex triangle logo are registered trademarks of Vertex Pharmaceuticals Incorporated.  
©2024 Vertex Pharmaceuticals Incorporated | 03/24



## Better Health, Brighter Future

Takeda is a global, R&D-driven biopharmaceutical company committed to discovering and delivering life-transforming treatments and vaccines that have a lasting impact on society.

Since our founding in 1781 in a market stall in Osaka, Japan, our values endure by putting patient needs first, building trust with society, strengthening our reputation, and developing the business - in that order.